International Journal of Microwave and Wireless Technologies, page 1 of 11.
doi:10.1017/S1759078711000122

Millimeter-wave interactions with the human body: state of knowledge and recent advances

MAXIM ZHADOBOV[1], NACER CHAHAT[1], RONAN SAULEAU[1], CATHERINE LE QUEMENT[2] AND YVES LE DREAN[2]

The biocompatibility of millimeter-wave devices and systems is an important issue due to the wide number of emerging body-centric wireless applications at millimeter waves. This review article provides the state of knowledge in this field and mainly focuses on recent results and advances related to the different aspects of millimeter-wave interactions with the human body. Electromagnetic, thermal, and biological aspects are considered and analyzed for exposures in the 30-100 GHz range with a particular emphasis on the 60-GHz band. Recently introduced dosimetric techniques and specific instrumentation for bioelectromagnetic laboratory studies are also presented. Finally, future trends are discussed.

Keywords: Millimeter waves, Biocompatibility, 60-GHz body-centric communications, BAN, Dosimetry, Dielectric properties, Bioelectromagnetics

Received 30 October 2010; Revised 17 January 2011

I. INTRODUCTION

Recent advances in millimeter-wave technologies have triggered an exponential interest to wireless applications at millimeter waves. Antennas and devices operating in this band have a reduced size compared to their counterparts in the lower part of the microwave spectrum. Furthermore, very high data rates (up to 4 Gb/s) can be reached for short- or long-range communications. The radio coverage strongly depends on frequency and is essentially determined by the water vapor and molecular oxygen-induced atmospheric absorptions. For instance, shifting the frequency from 70/80 to 60 GHz decreases the operating range from 3 km to 400 m [1]. This decrease is related to the 16 dB/km peak of oxygen-induced absorption around 60 GHz [2, 3] that makes this frequency range extremely attractive for secured local communications, particularly in indoor environments, guaranteeing low interference with other wireless services and devices, as well as with adjacent network cells. At the same time, because of this resonance absorption, human body has never been exposed to 57–64 GHz radiations in the natural environmental conditions.

60-GHz broadband short-range communications for wireless personal area networks have been promoted by the WirelessHD Interest Group and WiGig alliance. The current target market applications are mainly restricted to indoor wireless high-definition multimedia devices [4]. Integrated 60-GHz front-ends are expected to be commercialized by 2014 on lap tops. Moreover, recent progress in miniaturization and low-cost devices has triggered research activities aiming at developing future millimeter-wave body area networks (BAN). Recently, several world-leading research groups have focused on the characterization of the body channel, development of on-body antennas, and integration with already existing devices, e.g. [5].

Before being introduced on the market, millimeter-wave systems should comply with local regulations that are usually based on the ICNIRP and/or IEEE exposure limits. For far-field exposures, the power density (PD) averaged over 20 cm^2 is limited to 1 mW/cm^2 (general public) and to 5 mW/cm^2 (workers) in the 60-GHz band [6, 7]. To respect these limits and due to technological limitations, the typical power radiated by the radio front-ends is below 10 dBm. However, power densities up to 20 mW/cm^2 (general public) and 100 mW/cm^2 (workers) are permitted for local exposure scenarios, i.e. for PD averaged over 1 cm^2 [6]. Exposures under these conditions have had a limited practical interest so far, but should now be studied in detail due to the expected development of body-centric communication systems [5, 8, 9]. In such systems, the antennas might be placed directly on the body inducing localized exposures of the superficial body layers.

In this context, it is fundamental to analyze millimeter-wave/human body interactions from electromagnetic (EM) and thermodynamic viewpoints, as well as the potential biological consequences and their power thresholds.

The main purpose of this paper is to make an overview of the most recent results related to the different aspects of millimeter-wave interactions with the human body.

[1]Institute of Electronics and Telecommunications of Rennes (IETR), UMR CNRS 6164, University of Rennes 1, 11D, 263 av. du G. Leclerc, 35042 Rennes, France. Phone: + 33 2 23 23 67 06; Fax: + 33 2 23 23 69 69
[2]Intracellular Protein Homeostasis (HIP) from the UMR CNRS 6026, University of Rennes 1, Rennes, France
Corresponding author:
M. Zhadobov
Email: maxim.zhadobov@univ-rennes1.fr

II. INTERACTION OF THE MILLIMETER WAVES WITH THE HUMAN BODY

A) Primary biological targets for 60-GHz radiations

The primary biological targets of 60-GHz radiations are the skin and eyes. Exposure of the eyes leads to the absorption of the EM energy by the cornea characterized by a free water content of 75% and a thickness of 0.5 mm. Ocular lesions have been found after high-intensity exposure of an eye (3 W/cm^2, 6 min) [10]. However, studies performed at 60 GHz (10 mW/cm^2, 8 h) demonstrated no detectable physiological modifications [11], indicating that millimeter waves act on the cornea in a dose-dependent manner.

Hereafter we will essentially consider the interactions with the skin as it covers 95% of the human body surface. From the EM viewpoint, the skin can be considered as an anisotropic multilayer dispersive structure made of three different layers, namely, epidermis, dermis, and subcutaneous fat layer (Fig. 1). The skin also contains capillaries and nerve endings. It is mainly composed of 65.3% of free water, 24.6% of proteins, and 9.4% of lipids [12].

B) Dielectric properties

Knowledge of the dielectric properties of the skin is essential for the determination of the reflection from, transmission through, and absorption in the body, as well as for EM modeling. In contrast to frequencies below 20 GHz, existing data on the permittivity of tissues in the millimeter-wave band are very limited due to some technical difficulties. In the 10–100 GHz range, the dispersive dielectric properties of the skin and biological solutions are primarily related to the rotational dispersion of free water molecules. In particular, high losses are related to the free water relaxation with the peak at 19 GHz at 25°C [13].

The results of skin permittivity measurements reported in the literature so far have demonstrated strong correlation with the measurement technique and skin model (*in vivo* or *in vitro*, skin temperature, location on the body and thicknesses of different skin layers). Gabriel *et al.* [14] reported extrapolated complex permittivity of human skin up to 110 GHz based on measurements performed below 20 GHz. The results presented by Gandhi and Riazi [15] at 60 GHz were obtained using a Debye's model based on measurements performed for the rabbit skin at 23 GHz. Alabaster [16] measured the complex permittivity of excised human skin samples at millimeter waves using a free-space technique. Hwang *et al.* [17] completed *in vivo* measurement on human skin up to 110 GHz using a coaxial probe. Finally, Alekseev and Ziskin [18] carried out reflection measurement with an open-ended waveguide and proposed a homogeneous and multilayer human skin models fitting the experimental data.

The permittivity data available at 60 GHz are summarized in Table 1 for the room and body temperatures. The complex dielectric constant extracted from Gabriel's, Gandhi's, and Hwang's models at 55–65 GHz are presented in Fig. 2. These data are compared with the theoretical values obtained using Maxwell's mixture equation [19]. Significant discrepancies among the reported data are found for the real (11%) and imaginary (62%) parts (Gabriel's model is used as a reference).

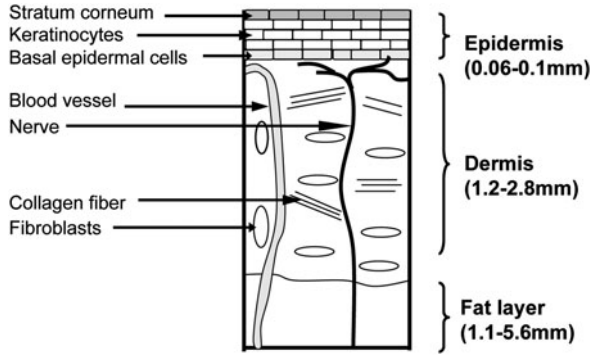

Fig. 1. Schematic representation of the skin structure.

C) Dosimetric quantities at millimeter waves

The major dosimetric quantities at millimeter waves are the following:

1) *Incident PD*: This is the main exposure characteristic adopted by most of the international guidelines and standards in the 10–300 GHz frequency range. The PD is defined as follows:

$$PD = \frac{P}{S} = |\vec{E} \times \vec{H}|, \tag{1}$$

where P is the incident power, S is the exposed surface area, and $\vec{E}$ and $\vec{H}$ are the electric and magnetic field vectors, respectively.

2) *Specific absorption rate (SAR)*: The SAR is a quantitative measure of power absorbed per unit of mass and time. In contrast to the PD, it also takes into account the physical properties of exposed samples:

$$SAR = \frac{P}{m} = \frac{\sigma|\vec{E}|^2}{\rho} = C\left.\frac{dT}{dt}\right|_{t=0}, \tag{2}$$

where m is the tissue mass, σ is its conductivity, and ρ is its mass density. C is the heat capacity, and T is the temperature. It is important to underline that in equation (2) σ combines both electrical and ionic conductivities.

3) Steady-state and/or transient temperature (T), which is particularly important in case of medium- and high-power exposures.

Table 1. Overview of the skin electrical properties at 60 GHz.

Reference	ε^*	T, °C	Method	Sample type
Gabriel [14]	$7.98 - j10.90$	37	E	*In vivo*
Gandhi [15]	$8.89 - j13.15$	37	E	*In vitro*
Hwang [17]	$8.05 - j4.13$	24–26	M	*In vivo*
Alabaster [16]	$9.9 - j9.0$	23	M	*In vitro*
Alabaster [16]	$13.2 - j10.3$	37	E	*In vitro*
Alekseev [18]	$8.12 - j11.14$	20–22	M	*In vivo*
Mixture eq. [19]	$9.38 - j12.49$	30	T	–

E, extrapolation; M, direct measurement; and T, theoretical value.

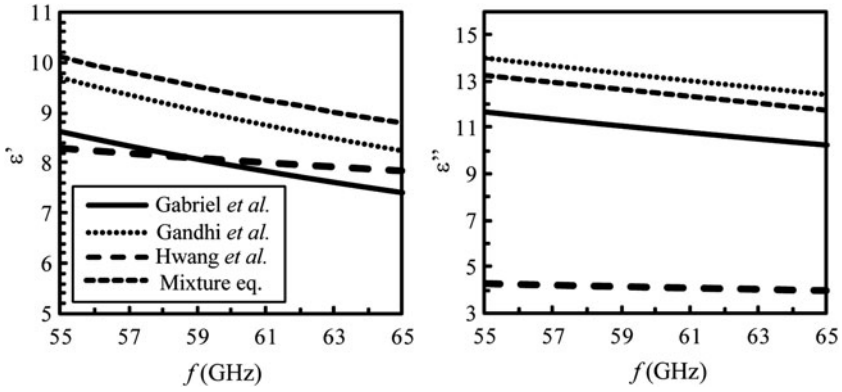

Fig. 2. Complex permittivity of the skin in 55–65 GHz range.

D) Reflection and transmission at the air/skin interface

The skin dielectric properties have a significant influence on the reflection and transmission at the air/skin interface. Their variability should be carefully taken into account for the on-body channel modeling.

For a 60-GHz plane wave illuminating a homogeneous semi-infinite flat skin model, analytically calculated reflection and transmission coefficients are represented in Fig. 3 for the perpendicular polarization ($\vec{E}$ perpendicular to the plane of incidence, TE mode) and parallel polarization ($\vec{E}$ parallel to the plane of incidence, TM mode). As expected, the reflected power strongly depends on the angle of incidence and polarization. For normal incidence, 30–40% of the incident power is reflected from the skin.

E) Absorption in the skin

The transmitted power decreases exponentially in the skin as a function of depth. The attenuation of the PD and SAR at 60 GHz are plotted in Fig. 4. The PD and SAR are maximal at the skin surface (Table 2). 40% (for Gabriel and Gandhi models) and 60% (for Hwang model) of the incident power reach dermis; only 0.1% (for Gabriel and Gandhi models) and 10% (for Hwang model) reach the fat layer. These results suggest that only epidermis and dermis should be considered for the EM dosimetry and on-body antenna characterization. This conclusion was confirmed by detailed analysis performed by Alekseev *et al.* [20] for multilayer skin models.

F) Influence of clothing

For future body-centric applications, it is particularly important to assess the effect of clothing on the millimeter-wave

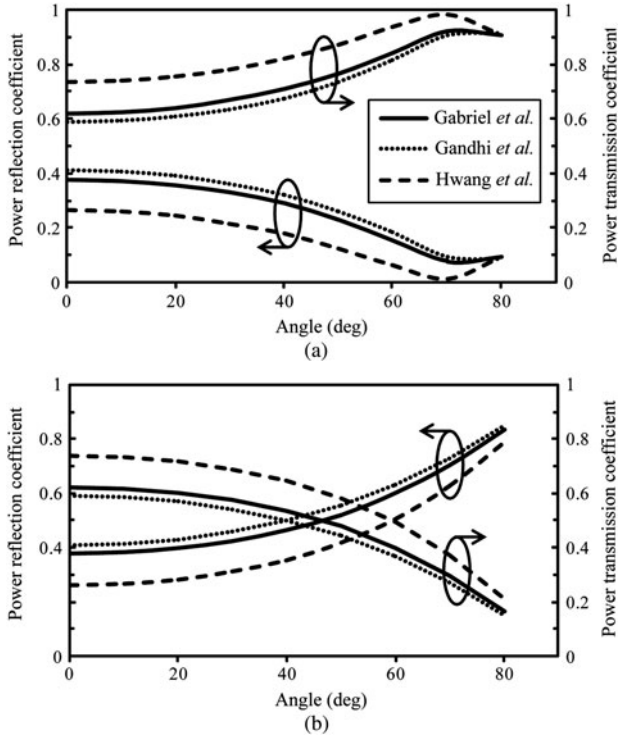

Fig. 3. Power reflection and transmission coefficients at the air/skin interface at 60 GHz for (a) parallel polarization and (b) perpendicular polarization.

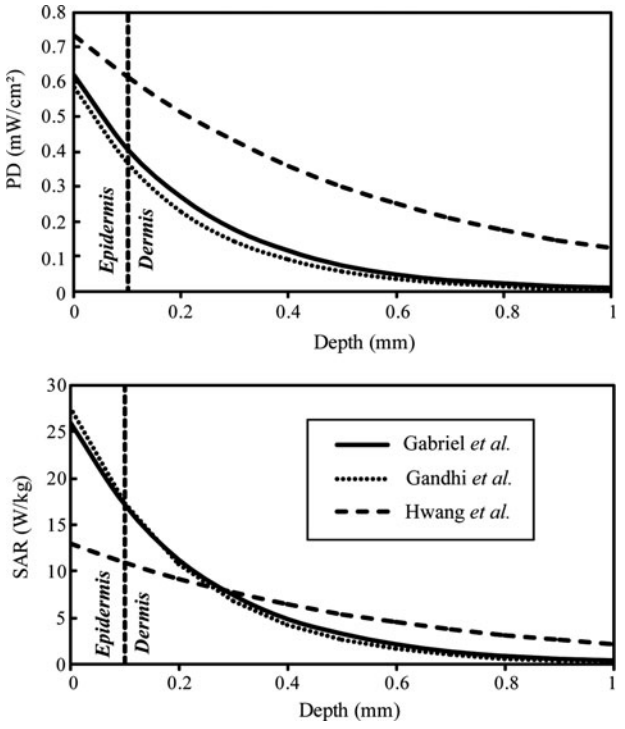

Fig. 4. Attenuation of the PD and SAR in the skin for an incident PD of 1 mW/cm^2 at 60 GHz.

Table 2. PD and SAR in the skin for different dielectric models (incident PD = 1 mW/cm²).

Model	Max. PD, *mW/cm²*	Max SAR, *W/kg*
Gabriel [14]	0.62	26.0
Gandhi [15]	0.59	27.6
Hwang [17]	0.74	13.1

absorption. The dielectric constant of clothing ε_c has never been investigated at 60 GHz. Here we assumed $\varepsilon_c = 1.25 + j0.024$; this corresponds to the complex permittivity of the dry fleece at microwave frequencies [21]. Since the clothing thickness d_c typically ranges between 0 and 1.2 mm, we computed the transmission coefficient at 60 GHz for this range using Gabriel's permittivity model [14]. The results show that the transmission coefficient slightly increases with the clothing thickness (Fig. 5).

Furthermore, to assess the contribution of an air gap d_a between the skin and clothing, we computed the power transmission coefficient for a four-layer model (Fig. 6). For a separation ranging from 0 to 2 mm, this coefficient varies from 56 to 72% with a minimum at 1.25 mm. These results demonstrate that, in contrast to the clothing that can enhance the transmission, the presence of an air gap induces a decrease of the power transmitted to the skin.

G) Millimeter-wave heating

Shallow penetration depth of 60-GHz radiations in the skin (typically 0.5 mm) results in SAR levels that are significantly higher than those obtained at microwaves for identical PD values. This may lead to a significant heating, even for low-power exposures. The steady-state distribution of the relative temperature increments for a PD of 1 and 5 mW/cm² is represented in Fig. 7. These results correspond to the analytical solution of the 1-D heat transfer equation that takes into account the effect of surface cooling and blood flow [22]. It is worthwhile to note that the heating is strongly correlated with the coefficient characterizing the heat transfer from the skin to air. These results demonstrate that heating due to local millimeter-wave exposure affects not only skin, but also subcutaneous tissues including fat and muscles. Therefore, a multilayer model should be used for the accurate assessment of the thermal effects.

The parametric study performed by Kanezaki *et al.* [23] demonstrated that the temperature distribution induced by a millimeter-wave exposure strongly depends on the geometrical and thermal properties of the multilayer model. Furthermore, Alekseev and Ziskin [24, 25] demonstrated that heating is related to the blood flow in the skin, i.e. to the environmental temperature and physiological conditions. It was shown that depending on these parameters steady-state temperature increments may vary by a factor of 3.

Finally, it is important to underline that temperature increments induced by the PD below current international exposure limits [6] are much lower than environmental thermal fluctuations.

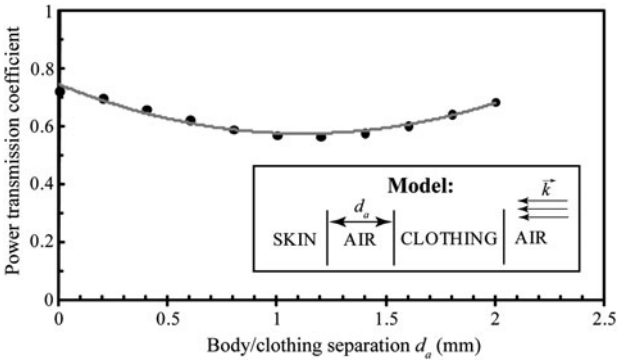

Fig. 6. Power transmission coefficient as a function of the air gap for $d_c = 1.25$ mm at 60 GHz.

III. INSTRUMENTATION AND DOSIMETRY FOR THE BIOCOMPATIBILITY STUDIES AT MILLIMETER WAVES

Nowadays, there is an increasing interest of the scientific community to the potential biological effects of millimeter waves [1]. The mechanisms of potential bioelectromagnetic interactions are not fully understood. Progress in this direction may result in new applications, but also in update of current exposure safety standards.

A) Exposure systems

Specific exposure systems have been used to experimentally investigate possible biological impacts of millimeter-wave exposures. Most of these systems can be divided in three

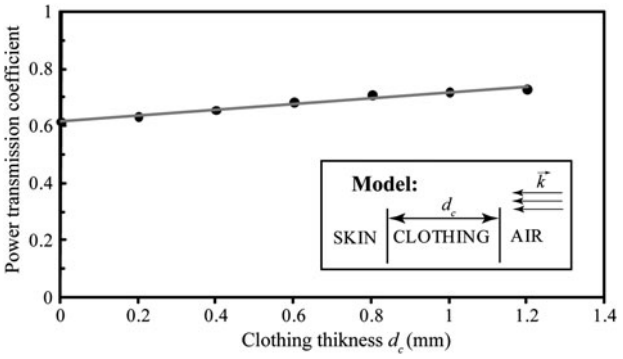

Fig. 5. Comparison of the transmission coefficient with and without clothing at 60 GHz.

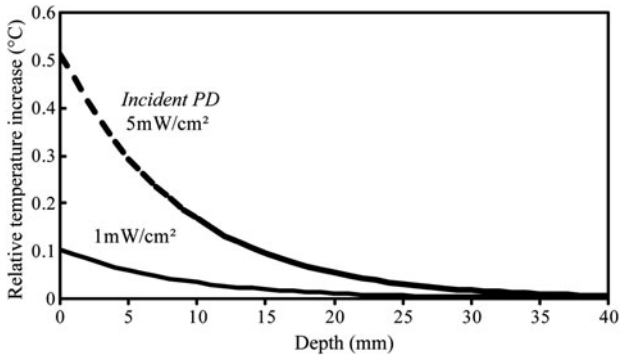

Fig. 7. Temperature increments for a homogeneous skin model exposed to a plane wave at 60 GHz.

main sub-units: (1) signal generation sub-unit; (2) spectrum and power control sub-unit; and (3) exposure chamber containing biological samples (Fig. 8).

The first sub-unit typically consists of a generator, amplifiers, isolator, attenuator, and radiating structure/antenna (e.g. [26]). The state of the art power limits are delivered by military systems (up to several MW at 94 GHz) [27]; however, the output power of the generators used for the research purposes at 60 GHz is typically limited to several watts [26, 28, 29].

The second sub-unit ensures real-time monitoring of the signal spectrum and output power stability that might be critical for the reliable interpretation of the biological outcome. It consists of a network analyzer, spectrum analyzer, and/or power meter.

Finally, the exposure chamber ensures appropriate environmental conditions for the biological samples under test and determines the EM boundary conditions. The requirements on the environmental conditions depend on the sample type. Biophysical samples, as for instance artificial models of biological membranes [30], require high purity of the air and absence of vibrations. For cells in culture, precise temperature control ($37 \pm 1^{\circ}$C) and CO_2 concentration of 5% must be ensured. The most commonly used animal models (e.g. mice, rats, rabbits [31]) require air circulation, lighting, and minimization of presence of additional environmental stresses.

Free-space exposure set-ups or anechoic chambers have been previously used in most of the studies implying cell or animal exposures to millimeter waves [32–35]. Recently, several research projects have been focused on the development of compact millimeter-wave reverberation chambers providing uniform exposure of animals independently on their position.

B) Dosimetry

Dosimetry studies have to be conducted to control and characterize the exposure levels within the samples and to optimize the exposure conditions (uniformity of the field distribution, number of simultaneously exposed samples, etc.). Two complementary approaches have been implemented.

1) NUMERICAL DOSIMETRY

A flowchart illustrating the general principle of the numerical *E*-field-based dosimetry for bioelectromagnetic studies is presented in Fig. 9. The major challenges for numerical dosimetry at millimeter waves are the following: (1) electrically large problems (λ_{skin} varies from 2.5 to 1.25 mm in 30–100 GHz range; this implies small mesh cell sizes of the numerical models – in the order of 0.1 mm [26]), (2) uncertainties on the precise values of the dielectric properties of tissues and absence of well-established database beyond 20 GHz [14], and (3) multi-scale problems related to the presence of the electrically small sub-structures (e.g. cell monolayers or different layers of skin [19]). Furthermore, the EM problem should be coupled with the thermodynamic one to carefully take into account possible heating and dielectric constant variations related to the thermal gradients [36]. Significant changes of permittivity values of biological tissues and solutions typically appear for the temperature gradients $\Delta T > 3^{\circ}$C.

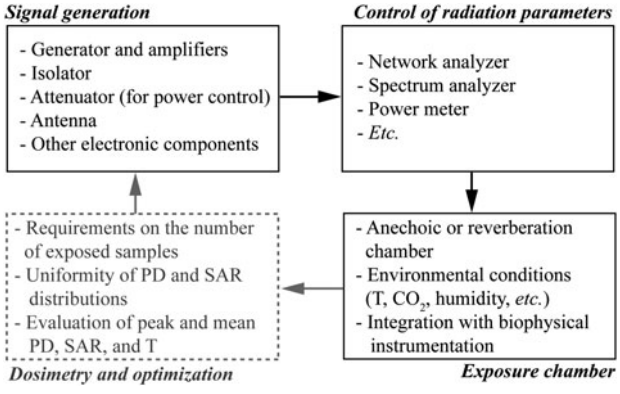

Fig. 8. Schematic representation of a typical millimeter-wave exposure system structure for laboratory studies.

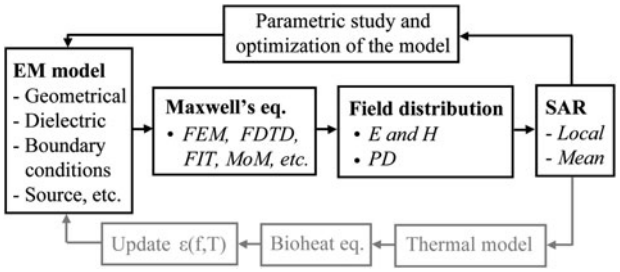

Fig. 9. Schematic representation of the numerical dosimetry approach at millimeter waves.

2) EXPERIMENTAL DOSIMETRY

At millimeter waves, the direct field-based dosimetry faces two major problems. First, the gradients of PD and SAR values within biological tissues are high because of the strongly localized absorption. This implies that the measurements should have spatial resolution better than 0.1–0.2 mm. Second, the already-existing *E*-field probes are too big in size for the local dosimetry [37], and additionally may perturb the EM field and temperature distribution. Furthermore, the sample conductivity should be known to determine the local or average SAR. Therefore, this experimental technique has a limited practical interest.

An alternative solution consists in remotely or invasively measuring the near-surface thermal dynamics of the sample under test (2). This is the most efficient way to experimentally determine the SAR and *T* distributions. Some non-perturbing techniques have been reported for the simultaneous determination of *T* and SAR, including optical fiber measurements [38], high-resolution infrared imaging [19], and utilization of thermosensitive liquid crystals [39].

C) Far-field exposures

In most of the reported *in vitro* studies, a directive antenna is used for the exposure of biological samples under free-space conditions or within a thermo-controlled incubator [26, 30, 33]. In this configuration, several samples can be exposed simultaneously with a sufficient uniformity of the PD distribution (typically better than 30%) and low peak-to-mean PD ratio. The detailed analysis of the PD and SAR distribution within the sample under test is performed using numerical techniques assuming the incident wave to be a normally incident

plane wave [40]. Finite-difference time-domain (FDTD), finite element method (FEM), and finite integration technique (FIT) have been successfully applied for the numerical dosimetry studies [19, 40]. This numerical modeling strategy was validated experimentally using infrared thermometry [19]. It is worthwhile to note that the meniscus effect, considered as an important factor for frequencies around 1 GHz [41], can be neglected in bioelectromagnetic studies at millimeter wave.

Several far-field exposure scenarios have also been reported for *in vivo* studies [11, 31, 42–44]. Here again, the choice of the far-field exposure conditions was motivated by the more uniform PD distribution compared to near-field exposures. Significant efforts have been undertaken by Alexeev *et al.* to supply accurate analytical, numerical, and experimental dosimetry for both animal and human skin exposures [20, 24, 25, 45]. Infrared radiometry in combination with microencapsulated thermosensitive liquid crystals was efficiently used for the EM and thermal dosimetry of rabbit and primates eyes [11, 39].

D) Near-field exposures

The major disadvantage of the far-field exposure systems is their low exposure efficiency (typically 10–15%) resulting in low PD levels on the biological samples. For a given antenna, there are two possible solutions to reach higher PD: (1) to increase the output power and (2) to bring closer the antenna and the sample. The first solution requires the use of high-power generators [43, 44] that are not always available for research purposes [46, 47]. The second solution implies characterization of the near-field distribution in the presence of biological samples in the reactive zone [38]. It was demonstrated that accurate dosimetry is crucial, as significant variations in T and SAR profiles appear for the displacements of the order of 0.5 mm under near-field exposure conditions [48].

A few near-field configurations have been implemented mainly in studies dealing with the potential therapeutic applications of millimeter waves including exposures at 61 GHz [24]. An experimental approach based on a high-resolution infrared imaging has shown to be highly effective for *in vivo* dosimetry applications [28, 48], but also for antenna measurements including determination of the near-field PD distribution [49]. Near-field exposures were also developed in a number of *in vitro* studies providing PD up to 100 mW/cm² at 60 GHz [35, 37, 46, 50].

IV. BIOLOGICAL EFFECTS OF MILLIMETER WAVES

There is a growing concern about possible health and biological effects of wireless technologies. Most of the bioelectromagnetic studies have investigated mobile phone exposures, and only few studies have focused on the biocompatibility of millimeter waves. Studies performed before 1998 were summarized by Pakhomov *et al.* [51]. In this paper we focus on major studies, essentially at 60 GHz, published after 1998.

Millimeter waves are non-ionizing radiations with a quantum of energy of 1.2×10^{-4}–1.2×10^{-3} eV. This energy is not sufficient to break chemical bonds as the energy required to induce ionization is of several orders of magnitude higher (typically 10 eV). However, some processes require much less energy to be altered, for instance the energy required for excitation of rotational modes is 10^{-5}–10^{-2} eV.

At 10–100 GHz, heating is the major effect resulting from the absorption of the EM energy. Significant thermal responses ($\Delta T > 0.5^{\circ}$C) appear after exposure to PD > 5 mW/cm², and, in case of very high-power exposures (above several hundreds of mW/cm²), it can lead to a pain sensation or tissue damage. The expected PD values for the emerging wireless communication systems are low enough to do not induce any biologically significant thermal effect typically appearing for the temperature increments exceeding 1–2°C [9]. The absence of direct or combined biological effects that do not directly depend on temperature rise is still controversial.

An argument in favor of possible interactions of millimeter waves with living organisms is their therapeutic applications introduced in some Eastern European countries more than 20 ears ago [52]. It is still unclear if the observed effects can be fully explained in the framework of the thermodynamics, or if direct EM interference with biological processes might also take place. It is important to underline that, in general, this therapeutic technique is not accepted by the Western medical community.

A) Biological effects at physiological levels

Most of the previous studies related to the interaction of millimeter waves with biological tissues were motivated by their potential therapeutic applications. The operating frequencies and power densities used for these applications are within 42–61 GHz and 5–15 mW/cm² ranges, respectively. According to the scientific literature, millimeter-wave action could have two main pathways: (1) analgesic effect and (2) effect on the inflammatory and immune systems (Table 3).

1) STUDIES OF ANALGESIC/HYPOALGESIC EFFECTS

Application of millimeter waves for the pain therapy showed some positive results [53]. Studies on animals demonstrated that the optimal effect was obtained at 61.22 GHz and 13.3 mW/cm² [54]. Various scientific publications reported positive data using blind tests with animal or volunteer studies. A 15-min exposure allows mice to better withstand noxious stimulation caused by the cold water tail-flick test [55, 56]. The hypoalgesic effect is not observed for PD < 0.5 mW/cm² [56]. Pretreatment with specific opioid

Table 3. Summary of the main reported biological effects.

Application	*f*, GHz	PD, mW/cm²	Biological response
Military	94	>1000	Strong thermal effect
Therapeutic	42.2	5 to 15	Hypoalgesic effects
	53.6		Effect on immune and inflammatory systems
	61.2		
Wireless communications	60	<5	Controversial effect on cellular proliferation
			No effect on gene expression related to cellular stress
			Possible effect on bio-membrane organization

antagonists completely blocked this effect [57] that suggests involvement of endogenous opioids (natural molecules involved in pain tolerance).

Taking into account local energy absorption, the most intriguing question is the link of observed effects with the exposure site. Hypoalgesic effects were found in animals and humans exposed at the acupuncture points [58–60]. Moreover, it was found that the most pronounced results were obtained by exposing the skin areas with the high nerve endings concentration [61] confirming the role of the peripheral neural system. Stimulation of the neurons located in skin induces a coordinated set of physiologic actions called systemic response (Fig. 10).

Two models could explain the therapeutic effects of millimeter waves: (1) direct activation of skin cells (keratinocytes and/or mastocytes) that induces the secretion of molecular signaling factors in the general blood circulation and (2) stimulation of the peripheral neural system that in turn activates the central neural system and induces the secretion of opioids peptides [54].

2) EFFECT ON INFLAMMATORY AND IMMUNE SYSTEM

During the past 25 years, the effects of millimeter waves on the immune system have been extensively studied, showing that they can modulate immune responses [52].

Szabo *et al.* analyzed the effect of 61.2-GHz exposure on epidermal keratinocytes by measuring the release of molecules playing a crucial role in cell trafficking in many physiological and pathological processes, so called chemokines (Fig. 10). In this work, the authors have found no modulation of production of the two chemokines involved in inflammatory skin diseases, namely RANTES (regulated on activation and normal T cell expressed and secreted) and IP-10 (interferon-gamma-inducible 10 kDa protein) [35, 62]. Nevertheless, they showed a modest increase in the intracellular level of IL-1β, a major pro-inflammatory cytokine produced and release by keratinocytes in response to various stimuli [62]. This result suggests that 61.2-GHz exposure could activate keratinocytes. Moreover, the *in vivo* study of Makar *et al.* [63, 64] on mice irradiated at 61.3 GHz and 31 mW/cm^2 also showed a pro-inflammatory effect initiated by activation of free nerve endings in the skin.

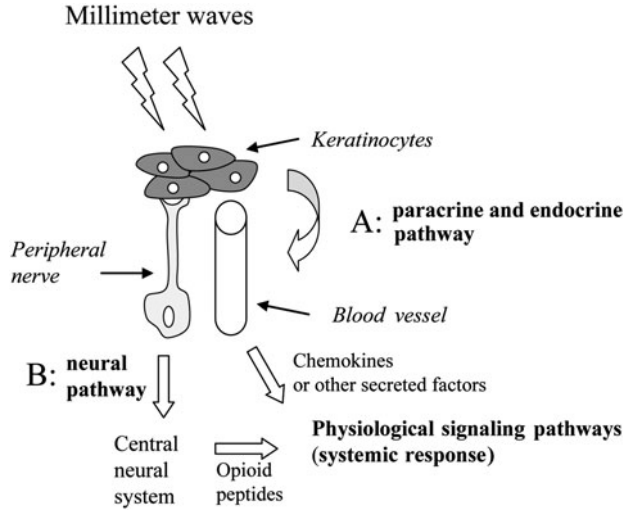

Fig. 10. Model illustrating possible mechanisms of millimeter-wave effects.

On the other hand, low-intensity 42-GHz exposure were described as displaying anti-inflammatory actions [65, 66]. Using a model of local acute inflammation in mice, Gapeyev *et al.* [42] have shown that millimeter waves reduces both the footpad edema and local hyperthermia induced by zymosan.

B) Biological effects at cellular and molecular levels

Cellular and sub-cellular experiments have been carried out in order to decipher the molecular mechanisms of possible millimeter-wave interactions. These studies are highly heterogeneous and few of them analyze common biological functions. However, three main topics can be extracted from the scientific literature: (1) effect on cell cycle and proliferation, (2) effect on gene expression, and (3) effect on biological membranes (Table 3).

1) EFFECT ON CELLULAR PROLIFERATION

Millimeter waves have been used in association with conventional drug therapy to treat skin melanoma [52] for investigating potential anti-proliferative effects. It was observed that 52–78 GHz exposure reduces the proliferation of human melanoma cells [67]. It was also shown that the inhibition of the proliferation was modest and correlated with structural changes and modification of the energy metabolism of the exposed cells [68]. However, 2 years latter, the same author failed to reproduce these results [69].

On the contrary, studies conducted by the authors' research team suggested that the proliferation was not significantly affected by low-power millimeter-wave exposure [26]. Results coming from Ziskin's research group demonstrated that the anti-cancer properties of millimeter waves may be indirect. It was found that exposure can reduce tumor metastasis through activation of natural killer cells [70], or protect cells from the toxicity of commonly used anticancer drugs [63].

2) EFFECT ON GENETIC EXPRESSION

According to the non-ionizing nature of the millimeter waves, most of the studies reported that they are not genotoxic [71]. On the other hand, the hypothesis of possible proteotoxic effect has been issued. Recently, our group published a thorough study showing that, if care is taken to avoid thermal effects, no notable change of protein chaperone expression, such as HSP70 or clusterin, could be detected [72]. These results are in agreement with previously reported data [35], which demonstrated the absence of the effect on the HSP induction. In order to further explore the potential proteotoxic effect of millimeter waves, we analyzed the effect on the reticulum stress and its associated unfolded protein response. Our results demonstrated that 59–61.2 GHz radiations at 0.14 mW/cm^2 do not affect the endoplasmic reticulum homeostasis [47, 73]. These data indicate that millimeter waves do not trigger an acute stress necessitating a transcriptional response.

3) EFFECT ON BIOMEMBRANES

Cell membrane consists of phospholipid bilayer with embedded proteins. Its structure is dynamic, although

highly ordered, and several studies suggested that it may be a molecular target of millimeter waves. For instance, data from our group showed that 60 GHz exposure at PD levels close to those typically expected from wireless communication systems (0.9 mW/cm^2) can induce structural modifications in artificial biomembranes [30]. The exposure reversibly increased the lateral pressure of the phospholipid monolayer, but this event is not strong enough to disturb the phospholipid microdomain organization within a biomembrane.

In parallel, it was demonstrated that structural changes in cellular membranes may occur during the exposure at 42.2 GHz (35.5 mW/cm^2) [74]. Reversible externalization of phosphatidylserine was observed without cellular damage that can eliminate the hypothesis of apoptosis induction. The biological relevance of this observation is not clear, but such a modification could play a role in the cellular signaling or cellular interactions. Moreover, it was demonstrated that 53-GHz radiations and 130-GHz pulse-modulated exposures can induce physical changes and modify permeability of phospholipid vesicles [75, 76]. It was assumed that millimeter waves could interfere with the orientation of charged and dipolar molecules leading to changes at the membrane/water interface.

V. CONCLUSION

This paper summarizes the most significant recent results and advances in the field of interaction of millimeter waves with the human body. EM, thermal, and biological aspects are reviewed with a particular emphasis on 60-GHz exposures. The recently introduced dosimetric techniques and instrumentation for bioelectromagnetic laboratory studies are presented.

First, available data on the dielectric properties of skin at 60 GHz is summarized demonstrating that well-established permittivity database is missing for the millimeter-wave band. It is shown that 26–41% of power is reflected at the air/skin interface for the normal incidence, and this value deviates significantly for illuminations under oblique incidence. More than 90% of the transmitted power is absorbed by the skin, and therefore single- or multi-layer skin model is sufficient for the reliable EM dosimetry. Clothing in direct contact with the skin enhances the power transmission, whereas an air gap of 0–2 mm between the clothes and skin decreases the transmission. Millimeter waves induce steady-state temperature increments of the order of several tenths of $^\circ$C for PD below the current far-field exposure limits; however, significant thermal effects may appear for local near-field exposures. It was demonstrated that, in contrast to the EM model, for the reliable thermal dosimetry, it is crucial to consider multi-layer structure including skin, fat, and muscle.

In addition, the state of the art in the development of laboratory exposure set-ups at millimeter waves, as well as in the numerical and experimental millimeter-wave dosimetry is provided in order to highlight the significant progress in this field during the last decade. An exhaustive analysis of the *in vitro* and *in vivo* biological studies is performed for the low- and high-power exposures. Whereas some effects have been observed for the medium-power exposures (5–15 mW/cm^2) leading to the local heating of the order of 1–2°C, most of the reproducible results for the lower PD demonstrated that direct biological effects at 60-GHz are not likely. Future trends of the bioelectromagnetic studies at millimeter waves cover such aspects as investigation of possible synergistic and combined EM/thermal effects, exact determination of power thresholds, and identification of possible biomarkers of the millimeter-wave exposure.

Finally, new trends in wireless BAN suggest that millimeter-wave on- and off-body sensors including wearable antennas are of increasing interest. To design appropriate antennas for these applications, the influence of the body on the antenna performances should be carefully taken into account. Therefore an accurate characterization of skin dielectric properties is required. Besides, one of the promising currently unexplored solutions to reduce susceptibility to shadowing is to implement reconfigurable millimeter-wave wearable antennas. For on-body applications, the characterization of the propagation channel is of utmost importance as it significantly differs from the free-space one, and no information is currently available in the scientific literature on this issue.

ACKNOWLEDGEMENTS

This work was supported by Agence Nationale de la Recherche (ANR), France, under ANR-09-RPDOC-003–01 grant (Bio-CEM project) and by "Centre National de la Recherche Scientifique (CNRS)", France.

REFERENCES

[1] Wells, J.: Faster than fiber: the future of multi Gb/s wireless. IEEE Microw. Mag., **10** (3) (2009), 104–112.

[2] Straiton, A.W.: The absorption and reradiation of radio waves by oxygen and water vapor in the atmosphere. IEEE Trans. Antennas Propag., **23** (1975), 595–597.

[3] Rosenkranz, P.W.: Shape of the 5 mm oxygen band in the atmosphere. IEEE Trans. Antennas Propag., **23** (1975), 498–506.

[4] Daniels, R.C.; Murdock, J.N.; Rappaport, T.S.; Heath, R.W.: 60 GHz Wireless: up close and personal. IEEE Microw. Mag., **11** (2010), 44–50.

[5] Hall, P.: Advances in antennas and propagation for body centric wireless communications, in European Conf. Antennas Propag. (EuCAP 2010), Barcelona, Spain, April 12–16, 2010.

[6] ICNIRP: Guidelines for limiting exposure to time varying electric, magnetic, and electromagnetic fields (up to 300 GHz). Health Phys., **74** (1998), 494–522.

[7] IEEE Std.: IEEE standard for safety levels with respect to human exposure to radio frequency electromagnetic fields, 3 kHz to 300 GHz. IEEE Std., C95.1, (2005).

[8] Xiao, S.-Q.; Zhou, M.-T.; Zhang, Y.: Millimeter Wave Technology in Wireless PAN, LAN, and MAN, CRC Press, Boca Raton, FL 33499, USA, 2008.

[9] Smulders, P.: Exploiting the 60 GHz band for local wireless multimedia access: prospects and future directions. IEEE Commun. Mag., **40** (2002), 140–147.

[10] Kojima, M. et al.: Acute ocular injuries caused by 60-Ghz millimeter-wave exposure. Health Phys., **97** (2009), 212–218.

[11] Kues, H.A.; D'Anna, S.A.; Osiander, R.; Green, W.R.; Monahan, J.C.: Absence of ocular effects after either single or repeated exposure to

10 mW/cm² from a 60 GHz CW source. Bioelectromagnetics, **20** (1999), 463–473.

[12] Duck, F.A.: Physical Properties of Tissue, Academic, Bath, UK, 1990. ISBN 0122228006.

[13] Ellison, W.J.: Permittivity of purewater, at standard atmospheric pressure, over the frequency range 0–25 THz and the temperature range 0–100°C. J. Phys. Chem. Ref. Data, **36** (2007), 1–18.

[14] Gabriel, S.; Lau, R.W.; Gabriel, C.: The dielectric properties of biological tissues: II Measurements in the frequency range 10 Hz to 20 GHz. Phys. Med. Biol., **41** (1996), 2251–2269.

[15] Gandhi, O.P.; Riazi, A.: Absorption of millimeter waves by human beings and its biological implications, IEEE Trans. Microw. Theory Tech., **34** (1986), 228–235.

[16] Alabaster, C.M.: Permittivity of human skin in millimetre wave band. Electron. Lett., **39** (2003), 1521–1522.

[17] Hwang, H.; Yim, J.; Cho, J.-W.; Cheon, C.; Kwon, Y.: 110 GHz broadband measurement of permittivity on human epidermis using 1 mm coaxial probe. IEEE Int. Micro. Symp. Digest, **1** (2003), 399–402.

[18] Alekseev, S.I.; Ziskin, M.C.: Human skin permittivity determined by millimeter wave reflection measurements. Bioelectromagnetics, **28** (2007), 331–339.

[19] Zhadobov, M.; Sauleau, R.; Le Dréan, Y.; Alekseev, S.I.; Ziskin, M.C.: Numerical and experimental millimeter-wave dosimetry for in vitro experiments. IEEE Trans. Microw. Theory Tech., **56** (2008), 2998–3007.

[20] Alekseev, S.I.; Radzievsky, A.A.; Logani, M.K.; Ziskin, M.C.: Millimeter-wave dosimetry of human skin. Bioelectromagnetics, **29** (2008), 65–70.

[21] Hertleer, C.; Tronquo, A.; Rogier, H.; Vallozzi, L.; Van Langenhove, L.: Aperture-coupled patch antenna for integration into wearable textile systems. IEEE Antennas Wirel. Propag. Lett., **6** (2007), 392–395.

[22] Foster, K.R.; Kritikos, H.N.; Schwan, H.P.: Effect of surface cooling and blood flow on the microwave heating of tissue. IEEE Trans. Biomed. Eng., **25** (1978), 313–316.

[23] Kanezaki, A.; Hirata, A.; Watanabe, S.; Shirai, H.: Parameter variation effects on temperature elevation in a steady-state, one-dimensional thermal model for millimeter wave exposure of one- and three-layer human tissue. Phys. Med. Biol., **55** (2010), 4647–4659.

[24] Alekseev, S.I.; Ziskin, M.C.: Influence of blood flow and millimeter wave exposure on skin temperature in different thermal models. Bioelectromagnetics, **30** (2009), 52–58.

[25] Alekseev, S.I.; Ziskin, M.C.: Millimeter-wave absorption by cutaneous blood vessels: a computational study. IEEE Trans. Biomed. Eng., **56** (2009), 2380–2388.

[26] Zhadobov, M. et al.: Evaluation of the potential biological effects of the 60-GHz millimeter waves upon human cells. IEEE Trans. Antennas Propag., **57** (2009), 2949–2956.

[27] Debouzy, J.C.; Crouzier, D.; Dabouis, V.; Malabiau, R.; Bachelet, C.; Perrin, A.: Biologic effects of millimeteric waves (94 GHz) are there long term consequences? Pathol. Biol., **55** (2007), 246–55.

[28] Kurogi, S.; Suzuki, Y.; Taki, M.: A novel in vitro exposure apparatus for 60 GHz millimeter-waves with post-wall waveguide, in Annual Meeting of BEMS, Seoul, June 14–18, 2010.

[29] Alekseev, S.I., Gordiienko, O.V.; Radzievsky, A.A.; Ziskin, M.C.: Millimeter wave effects on electrical responses of the sural nerve in vivo. Bioelectromagnetics, **31** (2010), 180–190.

[30] Zhadobov, M.; Sauleau, R.; Vié, V.; Himdi, M.; Le Coq, L.; Thouroude, D.: Interactions between 60 GHz millimeter waves and artificial biological membranes: dependence on radiation parameters. IEEE Trans. Microw. Theory Tech., **54** (2006), 2534–2542.

[31] Bellossi, A.; Dubost, G.; Moulinoux, J.; Ruelloux, M.; Himdi, M.; Rocher, C.: Biological effects of millimeter-wave irradiation on mice – preliminary results. IEEE Trans. Microw. Theory Tech., **48** (2000), 2104–2110.

[32] Chen, Q.; Zeng, Q.; Lu, D.; Chiang, H.: Millimeter wave exposure reverses TPA sup-pression of gap junction intercellular communications in HaCaT human keratinocytes. Bioelectromagnetics, **25** (2004), 2–4.

[33] Safronova, V.G.; Gabdoulkhakova, A.G.; Santalov, B.F.: Immunomodulating action of low intensity millimeter waves on primed neutrophils. Bioelectromagnetics, **23** (2002), 599–606.

[34] Szabo, I.; Rojavin, M.A.; Rojers, T.J.; Ziskin, M.C.: Reaction of keratinosytes to in vitro millimeter wave exposure. Bioelectromagnetics, **22** (2001), 358–364.

[35] Szabo, I.; Manning, M.R.; Radzievsky, A.A.; Wetzel, M.A.; Rojers, T.J.; Ziskin, M.C.: Low power millimeter wave irradiation exerts no harmful effect on human keratinocytes in vitro. Bioelectromagnetics, **24** (2003), 65–173.

[36] Cueille, M.; Collin, A.; Pivain, C.; Leveque, P.: Developement of a numerical model connecting electromagnetism, thermal and hydrodynamics in order to analyse in vitro exposure system. Ann. Telecommun., **63** (2008), 17–28.

[37] Pakhomov, A.G.; Prol, H.K.; Mathur, S.P.; Akyel, Y.; Campbell, C.B.G.: Search for frequency-specific effects of millimeter-wave radiation on isolated nerve function. Bioelectromagnetics, **18** (1997), 324–334.

[38] Zhadobov, M.; Sauleau, R.; Thouroude, D.; Nicolas Nicolaz, Ch.; Le Quément, C.; Le Dréan, Y.: Near-field electromagnetic dosimetry for in vitro studies at millimeter waves, in European Conf. on Antennas and Propagation (EuCAP 2010), Mo-17, Barcelone, Spain, April 2010.

[39] Suzuki, Y. et al.: Experimental analysis on the thermal convection of aqueous humor in anterior chamber driven by the millimeter-wave exposure at 77 GHz, in Annual Meeting of BEMS, Seoul, June 14–18, 2010.

[40] Zhao, J.X.; Wei, Z.: Numerical modeling and dosimetry of the 35 mm petri dish under 46 GHz millimeter wave exposure. Bioelectromagnetics, **26** (2005), 481–488.

[41] Schuderer, J.; Kuster, N.: Effect of the meniscus at the solid/liquid interface on the SAR distribution in petri dishes and flasks. Bioelectromagnetics, **24** (2003), 103–108.

[42] Gapeyev, A.B.; Mikhailik, E.N.; Chemeris, N.K.: Anti-inflammatory effects of low-intensity extremely high-frequency electromagnetic radiation: frequency and power dependence. Bioelectromagnetics, **29** (2008), 197–206.

[43] Jauchem, J.R.; Ryan, K.L.; Frei, M.R.: Cardiovascular and thermal responses in rats during 94 GHz irradiation. Bioelectromagnetics, **20** (1999), 264–267.

[44] Sypniewska, R.K.; Millenbaugh, N.J.; Kiel, J.L.; Blystone, R.V.; Ringham, H.N.; Mason, P.A.; Witzmann, F.A.: Protein changes in macrophages induced by plasma from rats exposed to 35 GHz millimeter waves. Bioelectromagnetics, **31** (2010), 656–663.

[45] Alekseev, S.I.; Gordiienko, O.V.; Ziskin, M.C.: Reflection and penetration depth of millimeter waves in murine skin. Bioelectromagnetics, **29** (2008), 340–344.

[46] Chen, Q.; Zeng, Q.L.; Lu, D.Q.; Chiang, H.: Millimeter wave exposure reverses TPA suppression of gap junction intercellular

communicationin HaCaT human keratinocytes. Bioelectromagnetics, **25** (2004), 1–4.

[47] Nicolas Nicolaz, Ch. et al.: Study of narrow band millimeter-wave potential interactions with endoplasmic reticulum stress sensor genes. Bioelectromagnetics, **30** (2009), 365–373.

[48] Suzuki, Y.; Shibuya, M.; Kurogi, S.; Taguchi, T.; Suzuki, Y.; Taki, M.: Millimeter-wave exposure apparatus with horn antenna and application to in vitro experiment, in Annual Meeting of BEMS, Seoul, June 14–18, 2010.

[49] Khizhnyak, E.P.; Ziskin, M.C.: Heating patterns in biological tissue phantoms caused by millimeter wave electromagnetic irradiation. IEEE Trans. Biomed. Eng., **41** (1994), 865–873.

[50] Yu, G. et al.: A study on biological effects of low-intensity millimeter waves. IEEE Trans. Plasma Sci., **30** (2002), 1489–1496.

[51] Pakhomov, A.G.; Akyel, Y.; Pakhomova, O.N.; Stuck, B.E.; Murphy, M.R.: Current state and implications of research on biological effects of millimeter waves: a review of the literature. Bioelectromagnetics, **19** (1998), 393–413.

[52] Rojavin, M.A.; Ziskin, M.C.: Medical applications of millimeter waves. Int. J. Med., **91** (1998), 57–66.

[53] Usichenko, T.I.; Edinger, H.; Gizhko, V.V.; Lehmann, C.; Wendt, M.; Feyerherd, F.: Low-intensity electromagnetic millimeter waves for pain therapy. Evid. Based Complement. Altern. Med., **3** (2006), 201–207.

[54] Radzievsky, A.A.; Gordiienko, O.V.; Alekseev, S.; Szabo, I.; Cowan, A.; Ziskin, M.C.: Electromagnetic millimeter wave induced hypoalgesia: frequency dependence and involvement of endogenous opioids. Bioelectromagnetics, **29** (2008), 284–295.

[55] Radzievsky, A.A.; Rojavin, M.A.; Cowan, A.; Alekseev, S.I.; Radzievsky, A.A. Jr.; Ziskin, M.C.: Peripheral neural system involvement in hypoalgesic effect of electromagnetic millimeter waves. Life Sci., **68** (2001), 1143–1151.

[56] Rojavin, M.A.; Radzievsky, A.A.; Cowan, A.; Ziskin, M.C.: Pain relief caused by millimeter waves in mice: results of cold water tail flick tests. Int. J. Radiat. Biol., **76** (2000), 575–579.

[57] Rojavin, M.A., Ziskin, M.C.: Electromagnetic millimeter waves increase the duration of anaesthesia caused by ketamine and chloral hydrate in mice. Int. J. Radiat. Biol., **72** (1997), 475–480.

[58] Lysenyuk, V.P.; Samosyuk, I.Z.; Kulikovich, Y.N.; Kozhanova, A.K.: Experimental study on the low-intensity millimeter-wave electromagnetic stimulation of acupuncture points. Acupunct. Electrother. Res., **25** (2000), 91–99.

[59] Vorobyov, V.V.; Khramov, R.N.: Hypothalamic effects of millimeter wave irradiation depend on location of exposed acupuncture zones in unanesthetized rabbits. Am. J. Chin. Med., **30** (2002), 29–35.

[60] Usichenko, T.I.; Ivashkivsky, O.I.; Gizhko, V.V.: Treatment of rheumatoid arthritis with electromagnetic millimeter waves applied to acupuncture points – a randomized double blind clinical study. Acupunct. Electrother. Res., **28** (2003), 11–18.

[61] Radzievsky, A.A.; Rojavin, M.A.; Cowan, A.; Alekseev, S.I.; Ziskin, M.C.: Hypoalgesic effect of millimeter waves in mice: dependence on the site of exposure. Life Sci., **66** (2000), 2101–2011.

[62] Szabo, I.; Rojavin, M.A.; Rogers, T.J.; Ziskin, M.C.: Reactions of keratinocytes to in vitro millimeter wave exposure. Bioelectromagnetics, **22** (2001), 358–364.

[63] Makar, V.; Logani, M.; Szabo, I.; Ziskin, M.: Effect of millimeter waves on cyclophosphamide induced suppression of T cell functions. Bioelectromagnetics, **24** (2003), 356–365.

[64] Makar, V.R.; Logani, M.K.; Bhanushali, A.; Alekseev, S.I.; Ziskin, M.C.: Effect of cyclophosphamide and 61.22 GHz millimeter waves on T-cell, B-cell, and macrophage functions. Bioelectromagnetics, **27** (2006), 458–466.

[65] Lushnikov, K.V.; Shumilina, Y.V.; Yakushina, V.S.; Gapeev, A.B.; Sadovnikov, V.B.; Chemeris, N.K.: Effects of low-intensity ultrahigh frequency electromagnetic radiation on inflammatory processes. Bull. Exp. Biol. Med., **137** (2004), 364–366.

[66] Gapeev, A.B.; Lushnikov, K.V.; Shumilina, Iu.V.; Chemeris, N.K.: Pharmacological analysis of anti-inflammatory effects of low-intensity extremely high-frequency electromagnetic radiation. Biofizika, **51** (2006), 1055–1068.

[67] Beneduci, A.; Chidichimo, G.; De Rose, R.; Filippelli, L.; Straface, S.V.; Venuta, S.: Frequency and irradiation time-dependant antiproliferative effect of low-power millimeter waves on RPMI 7932 human melanoma cell line. Anticancer Res., **25** (2005), 1023–1028.

[68] Beneduci, A.; Chidichimo, G.; Tripepi, S.; Perrotta, E.; Cufone, F.: Antiproliferative effect of millimeter radiation on human erythromyeloid leukemia cell line K562 in culture: ultra-structural- and metabolic-induced changes. Bioelectrochemistry, **70** (2007), 214–220.

[69] Beneduci, A.: Evaluation of the potential in vitro antiproliferative effects of millimeter waves at some therapeutic frequencies on RPMI 7932 human skin malignant melanoma cells. Cell. Biochem. Biophys., **55** (2009), 25–32.

[70] Logani, M.K.; Szabo, I.; Makar, V.; Bhanushali, A.; Alekseev, S.; Ziskin, M.C.: Effect of millimeter wave irradiation on tumor metastasis. Bioelectromagnetics, **27** (2006), 258–264.

[71] Vijayalaxmi; Logani, M.K.; Bhanushali, A.; Ziskin, M.C.; Prihoda, T.J.: Micronuclei in peripheral blood and bone marrow cells of mice exposed to 42 GHz electromagnetic millimeter waves. Radiat. Res., **161** (2004), 341–345.

[72] Zhadobov, M. et al.: Millimeter wave radiations at 60 GHz do not modify stress-sensitive gene expression of chaperone proteins. Bioelectromagnetics, **28** (2007), 188–196.

[73] Nicolas Nicolaz, C. et al.: Absence of direct effect of low-power millimeter-wave radiation at 60.4 GHz on endoplasmic reticulum stress. Cell. Biol. Toxicol., **25** (2009), 471–478.

[74] Szabo, I.; Kappelmayer, J.; Alekseev, S.I.; Ziskin, M.C.: Millimeter wave induced reversible externalization of phosphatidylserine molecules in cells exposed in vitro. Bioelectromagnetics, **27** (2006), 233–244.

[75] Ramundo-Orlando, A. et al.: The response of giant phospholipid vesicles to millimeter waves radiation. Biochim. Biophys. Acta, **1788** (2009), 1497–1507.

[76] Ramundo-Orlando, A. et al.: Permeability changes induced by 130 GHz pulsed radiation on cationic liposomes loaded with carbonic anhydrase. Bioelectromagnetics, **28** (2007), 587–598.

Maxim Zhadobov received the M.S. degree in radiophysics from Nizhni Novgorod State University, Russia, in 2003, and the Ph.D. degree in bioelectromagnetics from Institute of Electronics and Telecommunications of Rennes (IETR), France, in 2006. He accomplished post-doctoral training at the Center for Biomedical Physics, Temple University, Philadelphia, USA, in 2008 and then rejoined IETR as an Associate Scientist CNRS. His main scientific interests are in the field of biocompatibility of electromagnetic radiations, including interactions of microwaves, millimeter waves, and pulsed radiations at the cellular level, health risks, and environmental safety of emerging wireless

communication systems, biocompatibility of wireless biomedical techniques, therapeutic applications of non-ionizing radiations, bioelectromagnetic optimization of body-centric wireless systems, experimental and numerical electromagnetic dosimetry. Dr. Zhadobov was the recipient of the 2005 Best Poster Presentation Award from the International School of Bioelectromagnetics, 2006 Best Scientific Paper Award from the Bioelectromegnetics Society, and Brittany's Young Scientist Award in 2010.

Nacer Chahat graduated in electrical engineering and radio communications from the Ecole Supérieur d'ingénieurs de Rennes (ESIR), received the master's degree in telecommunication and electronics in 2009. Since 2009, he has been working toward the Ph.D. degree in signal processing and telecommunications at the Institute of Electronics and Telecommunications of Rennes (IETR), University of Rennes 1, Rennes, France. His current research fields are millimeter-wave antennas, and the evaluation of the interaction between the electromagnetic field and human body. He accomplished a 6-month master's training period as a special research student in 2009 at the Graduate School of Engineering, Chiba University, Chiba, Japan.

Ronan Sauleau graduated in 1995 from the "INSA de Rennes", Rennes, France. He joined the "Ecole Normale Supérieure de Cachan" in 1995 and received the "Agrégation" in 1996. He received the Ph.D. degree from the University of Rennes 1 in 1999. He received the "Habilitation à Diriger des Recherches" in November 2005 and is Full Professor since November 2009. His main fields of interest are millimeter-wave antennas, focusing devices, periodic structures (EBG materials and metamaterials), and biological effects of millimeter waves. He holds five patents and has coauthored 83 journal papers and more than 200 publications in national and international conferences. He received the 2004 ISAP Young Researcher Scientist Fellowship (Japan) and the first Young Researcher Prize in Brittany, France in 2001. In 2007, he was elevated as a Junior Member of the "Institut Universitaire de France". He received the Bronze Medal from CNRS in 2008.

Catherine Le Quément received the Ph.D. degree in biology from the University of Rennes 1, Rennes, France in 2008. From 2006 to 2008, she was an Associate Professor at the University of Rennes 1 (Attachée Temporaire d'Enseigment et de Recherche), where she taught pharmacology and biochemistry. Since 2008, she accomplishes post-doctoral training at the Cellular and Molecular Interactions lab, Rennes, France. Her main subject of interest is cell responses to environmental stress (cigarette smoke, eletromagnetic waves, etc.).

Yves Le Dréan received the Ph.D. degree and "Habilitation à Diriger des Recherches" in biology from the University of Rennes 1, Rennes, France in 1993 and 2007, respectively. He joined the hospital for sick children at Toronto, Canada, as a post-doctoral fellow in 1994. Since 1997, he has been an Associate Professor at the University of Rennes 1, where he teaches molecular biology and biochemistry. His main subject of interest is the control of genetic expression. His current research activities are related to the investigations of cell responses to proteotoxic stress. Since 2004 he has been also actively involved in the field of biological effects of electromagnetic waves.

Bioelectromagnetics 29:340–344 (2008)

Reflection and Penetration Depth of Millimeter Waves in Murine Skin

S.I. Alekseev, O.V. Gordiienko, and M.C. Ziskin*

Center for Biomedical Physics, Temple University Medical School, Philadelphia, Pennsylvania

Millimeter (mm) wave reflectivity was used to determine murine skin permittivity. Reflection was measured in anesthetized Swiss Webster and SKH1-hairless mice in the 37–74 GHz frequency range. Two skin models were tested. Model 1 was a single homogeneous skin layer. Model 2 included four skin layers: (1) the stratum corneum, (2) the viable epidermis plus dermis, (3) fat layer, and (4) muscle which had infinite thickness. We accepted that the permittivity of skin in the mm wave frequency range results from the permittivity of cutaneous free water which is described by the Debye equation. Using Fresnel equations for reflection we determined the skin parameters best fitting to the reflection data and derived the permittivity of skin layers. The permittivity data were further used to calculate the power density and specific absorption rate profiles, and the penetration depth of mm waves in the skin. In both murine models, mm waves penetrate deep enough into tissue to reach muscle. In human skin, mm waves are mostly absorbed within the skin. Therefore, when extrapolating the effects of mm waves found in animals to humans, it is important to take into account the possible involvement of muscle in animal effects. Bioelectromagnetics 29:340–344, 2008.

Key words: murine skin permittivity; millimeter wave dosimetry; skin modeling

INTRODUCTION

Therapeutic application of millimeter (mm) waves in medicine [Rojavin and Ziskin, 1998] has stimulated great interest in understanding the mechanisms of biological action of mm waves. Recently, mm wave effects on the immune system, tumor metastasis and mm wave induced hypoalgesia have been extensively studied in mice [Radzievsky et al., 2000, 2001, 2004; Makar et al., 2003, 2005; Lushnikov et al., 2004; Logani et al., 2006]. The reported actions arise from induced systematic effects that result from the shallow penetration of mm waves into the skin. To determine the primary targets for mm wave action, it is first necessary to determine what biological structures are within the penetration depth of mm waves. Furthermore, to extrapolate the biologic effects found in mice to humans, it is necessary to know the mm wave intensity distribution in both murine and human skin. Both of these tasks require accurate dosimetry. Dosimetry calculations are based primarily on the geometry and permittivity values of skin layers.

Recently we have reported the results of a study of human skin permittivity using mm wave reflectometry [Alekseev and Ziskin, 2007] and human skin dosimetry [Alekseev et al., 2008]. Permittivity was determined for both homogeneous and multilayer skin models.

We did not find in the literature any permittivity data specific for murine skin nor any detailed analysis of the mm wave interaction with murine skin. Therefore, the aims of the present study were to determine the permittivity of murine skin using mm wave reflectometry and to calculate the power density (PD) and specific absorption rate (SAR) profiles as well as penetration depth of mm waves in murine skin based on homogeneous and multilayer skin models. To evaluate the influence of hair on murine skin permittivity, we used hairy and hairless mice.

METHODS

Animals

Millimeter wave reflection was studied in two strains of mice: male Swiss Webster mice, body weight approximately 20–25 g (obtained from Taconic,

Grant sponsor: NIH NCCAM; Grant number: P01-AT002025.

*Correspondence to: M.C. Ziskin, Center for Biomedical Physics, Temple University Medical School, 3400 North Broad Street, Philadelphia, PA 19140. E-mail: ziskin@temple.edu

Received for review 9 August 2007; Final revision received 6 November 2007

DOI 10.1002/bem.20401
Published online 25 January 2008 in Wiley InterScience (www.interscience.wiley.com).

Germantown, NY) and female SKH1-hairless mice, body weight approximately 22–25 g (obtained from the Charles River Laboratories, Wilmington, MA). The animals were housed in plastic cages in the Central Animal Facility at Temple University. The Institutional Animal Care and Use Committee of Temple University approved the experimental protocols. All experiments were conducted under anesthesia with a mixture of ketamine (95 mg/kg), xylazine (10 mg/kg), and acepromazine (0.7 mg/kg). Reflection measurements were made on the caudal dorsum and flank areas of both strains of mice. On the Swiss Webster mice, these regions were shaved on the day preceding the measurements. We used 10 animals of both strains in each experiment.

Reflection Measurements

The methods and techniques used for mm wave reflection measurements were the same as described in our recent publication [Alekseev and Ziskin, 2007]. Reflection was measured at the open-ended waveguide applied to the caudal dorsum or flank area of murine skin in the 37–74 GHz frequency range. Reflection measurements were performed at ambient room temperature of 22–24 °C and relative humidity of 15–30%.

Measurements of Skin Temperature and Thickness

The skin temperature was measured using a thermocouple of the IT-23 type (Physitemp, Inc., Clifton, NJ) immediately before and after each reflection measurement. Average temperature of these two values was used for the permittivity calculation. The skinfold thickness was measured using a Starrett micrometer (L.S.Starrett Co., Athol, MA). To determine the thickness of skin, the skinfold thickness was divided by two. The skin thickness was also measured with the micrometer directly in euthanized mice. Both measurements gave the same result.

Skin Models

In modeling mm wave interaction with skin, we applied a homogeneous unilayer and a four layer skin model. The four layer model contained (1) the stratum corneum (SC), (2) the viable epidermis plus dermis, (3) fat layer, and (4) muscle which had infinite thickness. We made several assumptions. First, the skin layers used in both models were considered to have distinct plane boundaries. Second, the skin layers contained different amounts of free water. Third, permittivity of biological tissue, including skin, in the gigahertz frequency range results mostly from the polarization of free water molecules [Grant, 1982; Foster and Schwan, 1986; Gabriel et al., 1996a].

The permittivity of each skin layer (i) was described by the Debye equation with a single relaxation time τ equal to that of pure water at skin temperature:

$$\varepsilon_i^* = \varepsilon_{\infty i} + \frac{\Delta\varepsilon_i}{1 + j\omega\tau} + \frac{\sigma_i}{j\omega\varepsilon_o} \quad (1)$$

where $\omega = 2\pi f$, f is the frequency, $j = (-1)^{1/2}$, $\Delta\varepsilon_i = \varepsilon_{si} - \varepsilon_{\infty i}$ the magnitude of the dispersion of the free water fraction of the skin layer i, ε_{si} the permittivity at $\omega\pi \ll 1$, $\varepsilon_{\infty i}$ the optical permittivity, $\varepsilon_o = 8.85 \times 10^{-12}$ F/m, σ_i the skin ionic conductivity. The permittivities of the fat and muscle layers were selected in accordance with Gabriel et al. [1996b].

Fitting Procedure

To fit the theoretical equations for calculating the power reflection coefficient R in different models to the reflection experimental data, we used the least-squares technique. The standard deviation of the differences between the calculated values and the measured values in the final fit was used as a measure of goodness of fit.

The optical permittivity and ionic conductivity, and the thickness of the SC played an insignificant role in the fitting procedure. Taking into account that the optical permittivity of the solid fraction of skin and pure water were equal to 2.5 and 5.2, respectively, the optical permittivity for each skin layer was approximated as follows:

$$\varepsilon_{\infty i} = 2.5 + 2.7 w_{ti} \quad (2)$$

where w_{ti} is the weight fraction of the total water content of skin layer i. The weight fraction of total water was set equal to 0.33 for the SC [Imokawa et al., 1991] and 0.6 for the viable epidermis and dermis layer [Duck, 1990]. The ionic conductivities of the SC and the viable epidermis and dermis were set equal to 0 and 1.4 S/m, respectively [Alekseev and Ziskin, 2007].

In determining skin permittivity we varied two parameters, the permittivity increment $\Delta\varepsilon_i$, and the thickness d_i. The thickness of the SC was fixed equal to its typical literature value of 0.015 mm [Warner et al., 1988]. The thickness of the fat layer was determined as the difference between the total skin thickness measured experimentally and the thickness of the epidermis plus dermis.

A sensitivity analysis showed that a 10% variation in reflection measurements resulted in a variation of $\Delta\varepsilon_i$ within10% and d_i within15%. The least-squares fit was considered to be acceptable if the SD was no more than

±15%. The results of reflection measurements are presented as mean ± SD (n = number of independent experiments).

Calculation of mm Wave Power Deposition

Millimeter waves were considered to be at normal incidence to the skin surface. To calculate the power reflection coefficient (R) and power density profile PD(z) as a function of skin depth we applied the Fresnel equations [Born and Wolf, 1975; Alekseev and Ziskin, 2000, 2007]. The penetration depth δ was calculated as $\delta = c/\omega \cdot n''$ where c is the velocity of light.

RESULTS

The mean thickness of skin including the thickness of the fat layer in the caudal dorsum and flank areas was 0.37 ± 0.03 mm in the Swiss Webster mice and 0.38 ± 0.06 mm in the SKH1-hairless mice. The mean skin surface temperature at the same sites was 32.8 ± 0.4 °C in the Swiss Webster mice and 30.3 ± 0.5 °C in the SKH1-hairless mice.

The dependence of the power reflection coefficient measured in the hairy murine skin on frequency is shown in Figure 1. The difference between the reflection data obtained from the caudal dorsum or flank areas was statistically insignificant. Reflection from hairless mice was slightly greater than from hairy mice (≤7.4%). The data obtained from both strains of mice were well fitted to the homogeneous or multilayer skin models. The parameters of the homogeneous and multilayer skin models giving the best fit to the data are presented in Table 1. The electrical parameters of

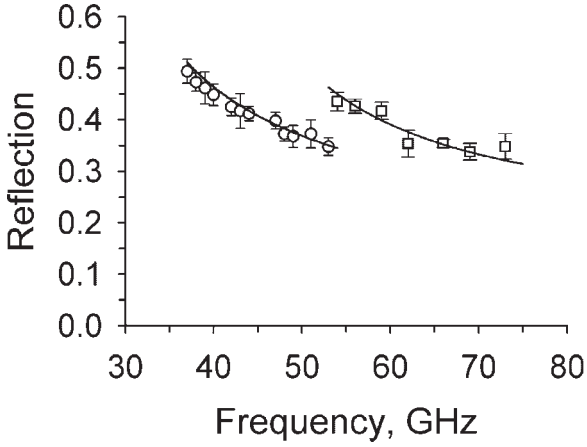

Fig. 1. Power reflection coefficient versus frequency for hairy murine skin. Symbols are experimental data. The error bars represent SD at $n = 10$. Solid lines are fits to the four layer skin model. Reflection curves for hairless murine skin were similar to those of hairy murine skin but the values of the power reflection coefficients were 6.3–7.4% higher.

TABLE 1. Parameters of Murine Skin Models Giving the Best Fit to the Experimental Reflection Data

	SKH1-hairless mice, model number		Swiss Webster (hairy) mice, model number	
Parameter	1	4	1	4
SC				
ε_∞	—	3.39	—	3.39
$\Delta\varepsilon$	—	0	—	0
d, mm	—	0.015[a]	—	0.015[a]
σ, S/m	—	0	—	0
$E^- + D$				
ε_∞	4.12	4.12	4.12	4.12
$\Delta\varepsilon$	18.82	27.21	16.10	24.87
d, mm	∞	0.25	∞	0.24
σ, S/m	1.4	1.4	1.4	1.4
Fat				
d, mm	—	0.13	—	0.13
Muscle				
d, mm	—	∞	—	∞
$\tau \times 10^{12}$, s[a]	7.14	7.14	6.9	6.9

The stratum corneum and the rest of epidermis plus dermis are denoted as SC and $E^- + D$, respectively; d is the thickness and σ is the ionic conductivity of the skin layer. In homogeneous skin (model 1), $E^- + D$ stands for the whole skin. Other symbols used in the table are given in the "Methods Section".
[a]Literature value.

Table 1 used with the Debye Equation (1) determine permittivity of the homogeneous skin or permittivity of skin layers in the multilayer skin model. They were further used to calculate the reflection, PD, and SAR profiles, and the penetration depth of mm waves in the skin.

The power reflection coefficient and penetration depth calculated for the plane mm waves at the therapeutic frequencies are given in Table 2. At each of three frequencies tested, the penetration depth of the hairy skin was 9.0–9.7% less than that of the hairless skin. Since the penetration depth is inversely proportional to attenuation, this result implies that hairless skin is approximately 9.5% more attenuating of mm waves than is hairy skin. The R and δ values can be used to evaluate SAR in homogeneous skin. Once the

TABLE 2. Power Reflection Coefficient and Penetration Depth of Plane Millimeter Wave Electromagnetic Field in Murine Skin at Therapeutic Frequencies

	Swiss Webster (hairy)		SKH1-hairless	
Frequency, GHz	R	δ (mm)	R	δ (mm)
42.25	0.32	0.93	0.34	0.85
53.57	0.29	0.79	0.31	0.72
61.22	0.27	0.73	0.29	0.67

Calculations were made using the homogeneous skin model.

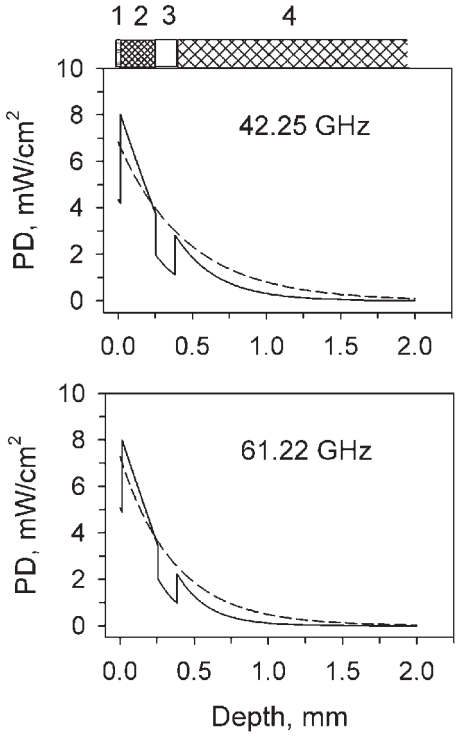

Fig. 2. Power density (PD) profiles within hairy murine skin calculated for 42.25 and 61.22 GHz using the one (dashed line) and four (solid line) layer skin models. In the four layer model, 1 denotes the SC, 2 is the viable epidermis plus dermis, 3 is the fat layer, and 4 is the muscle. Calculations were made for the plane wave at the incident PD of 10 mW/cm^2. The PD profiles within the hairless murine skin were close to those shown on the graph.

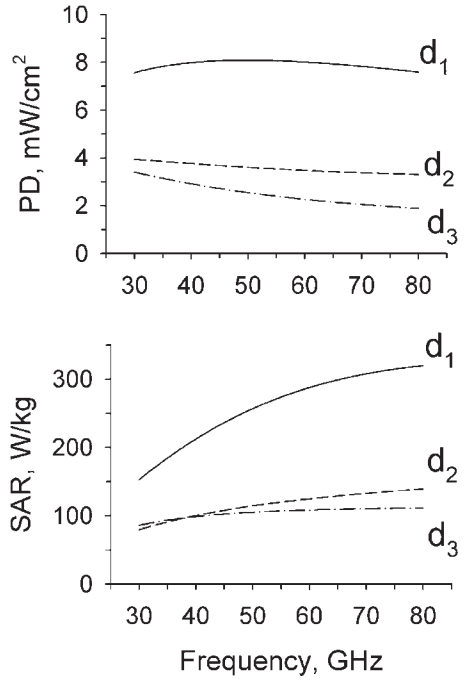

Fig. 3. Frequency dependence of the PD and SAR at a depth of d_1 (the front surface of the viable epidermis), d_2 (the rear surface of the dermis), and d_3 (the front surface of the muscle) of the hairy murine skin. Calculations were made for a plane wave at the incident PD of 10 mW/cm^2.

incident PD, I, is defined the SAR at a depth of z can be calculated as follows [Gandhi and Riazi, 1986]:

$$\mathrm{SAR}(z) = \frac{2(1-R)I}{\rho\delta} e^{-2z/\delta} \qquad (3)$$

The results of calculation of the PD profiles for the two therapeutic frequencies 42.25 and 61.22 GHz in hairy murine skin are shown in Figure 2. The PD profiles obtained for the hairless murine skin showed little difference. Millimeter waves penetrated deep enough to reach the muscle, that is, 42.5% and 32% of mm wave energy entering the skin at 42.25 and 61.22 GHz, respectively, was absorbed within the muscle. In the skin layers with lower water content, that is, with the higher wave impedances, the SC and fat, the PD was lower than in the viable epidermis and muscle, respectively.

The changes of the PD with frequency in the different layers of skin were small (Fig. 3). The SAR values increased notably with the frequency at the surface of the viable epidermis. At the surface of the deeper muscle layer and at the rear surface of the dermis, the SAR values were close to each other. At both regions the changes of SAR with frequency were not as pronounced as on the epidermal layer.

DISCUSSION

In modeling the mm wave interaction with murine skin we used plane wave exposure and simplified skin models. The heterogeneity within each skin layer and non-parallel internal boundaries would affect the calculated results. However, we do not expect a significant influence of these factors on the PD deposition in the skin and underlying tissue as the heterogeneous and multilayer models resulted in similar results. This can be explained by the small difference in water content of different tissue layers except for the SC and fat layers. The thin SC and fat layers produced a small effect on the PD deposition [Alekseev et al., 2008].

Reflection from both hairy and hairless murine skin was lower than from human skin [Alekseev and Ziskin, 2007]. This result can be explained by the lower free water content of murine skin in comparison with human skin.

We found that hairy skin, even when shaved, reflected mm waves less than hairless skin. This could be due to the lower free water content of hairy skin resulting from the presence of hair left in the skin after shaving. Hair does not contain free water [Lynch and Marsden, 1969] and occupies some skin volume thereby decreasing the effective free water content of the skin. To some extent, our calculations supported this hypothesis showing that the volume fraction of free water in hairless murine skin was about 11% higher than in hairy skin. The same influence of hair on skin water content could be expected in human skin in sites with marked hair presence.

The calculations of the PD and SAR profiles in murine skin revealed that mm waves reach the muscle layer of mice. Hence, in addition to the epidermis and dermis cells, mm waves may affect the structures located in the fat and muscle layers. However, in human skin mm waves are mostly absorbed within the skin (99.1% and 99.7% of energy entering the skin at 42.25 and 61.22 GHz, respectively) [Alekseev et al., 2008]. Therefore, when extrapolating the effects of mm waves found in animals to humans, it is important to determine the location of the biological structures affected by mm waves. If the primary target of mm wave action in mice is located, for example, in muscle then we cannot extrapolate this effect to humans. Thus, to make adequate extrapolations from animal to humans it is important to take into account the difference in the PD and SAR distributions in animal and human skin.

REFERENCES

Alekseev SI, Ziskin MC. 2000. Reflection and absorption of millimeter waves by thin absorbing films. Bioelectromagnetics 21:264–271.

Alekseev SI, Ziskin MC. 2007. Human skin permittivity determined by millimeter wave reflection measurements. Bioelectromagnetics 28:331–339.

Alekseev SI, Radzievsky AA, Logani MK, Ziskin MC. 2008. Millimeter wave dosimetry of human skin. Bioelectromagnetics 29:65–70.

Born M, Wolf E. 1975. Principles of optics. Electromagnetic theory of propagation, interference and diffraction of light. Oxford, UK: Pergamon Press. pp 627–631.

Duck FA. 1990. Physical properties of tissue. A comprehensive reference book. San Diego, CA: Academic Press, Inc. pp 319–328.

Foster KR, Schwan HP. 1986. Dielectric properties of tissues. In: Polk C, Postow E, editors. CRC handbook of biological effects of electromagnetic fields. Boca Raton, FL: CRC Press, Inc. pp 27–96.

Gabriel C, Gabriel S, Corthout E. 1996a. The dielectric properties of biological tissues: I. Literature survey. Phys Med Biol 41: 2231–2249.

Gabriel S, Lau RW, Gabriel C. 1996b. The dielectric properties of biological tissues: III. Parametric models for the dielectric spectrum of tissues. Phys Med Biol 41:2271–2293.

Gandhi OP, Riazi A. 1986. Absorption of millimeter waves by human beings and its biological implications. IEEE Trans Microwave Theory Tech 34:228–235.

Grant EH. 1982. The dielectric method of investigating bound water in biological material: An appraisal of the technique. Bioelectromagnetics 3:17–24.

Imokawa G, Kuno H, Kawai M. 1991. Stratum corneum lipids serve as a bound-water modulator. J Invest Dermatol 96:845–851.

Logani MK, Szabo I, Makar V, Bhanushali A, Alekseev S, Ziskin MC. 2006. Effect of millimeter wave irradiation on tumor metastasis. Bioelectromagnetics 27:258–264.

Lushnikov KV, Shumilina YV, Yakushina VS, Gapeev AB, Sadovnikov VB, Chemeris NK. 2004. Effects of low-intensity ultrahigh frequency electromagnetic radiation on inflammatory processes. Bull Exp Biol Med 137:364–366.

Lynch LJ, Marsden KH. 1969. NMR of absorbed systems. II. A NMR study of keratin hydration. J Chem Phys 51:5681–5691.

Makar V, Logani M, Szabo I, Ziskin M. 2003. Effect of millimeter waves on cyclophosphamide induced suppression of T cell functions. Bioelectromagnetics 24:356–365.

Makar V, Logani MK, Bhanushali A, Kataoka M, Ziskin MC. 2005. Effect of millimeter waves on natural killer cell activation. Bioelectromagnetics 26:10–19.

Radzievsky AA, Rojavin MA, Cowan A, Alekseev SI, Ziskin MC. 2000. Hypoalgesic effect of millimeter waves in mice: Dependence on the site of exposure. Life Sci 66:2101–2111.

Radzievsky AA, Rojavin MA, Cowan A, Alekseev SI, Radzievsky AA, Jr., Ziskin MC. 2001. Peripheral neuronal system involvement in hypoalgesic effect of electromagnetic millimeter waves. Life Sci 68:1143–1151.

Radzievsky AA, Gordiienko OV, Szabo I, Alekseev SI, Ziskin MC. 2004. Millimeter wave induced suppression of B16F10 melanoma growth in mice: Involvement of endogenous opioids. Bioelectromagnetics 25:466–473.

Rojavin MA, Ziskin MC. 1998. Medical application of millimeter waves. Q J Med 91:57–66.

Warner RR, Myers MC, Taylor DA. 1988. Electron probe analysis of human skin: Determination of the water concentration profile. J Invest Dermatol 90:218–224.

Bioelectromagnetics 24:165–173 (2003)

Low Power Millimeter Wave Irradiation Exerts No Harmful Effect on Human Keratinocytes In Vitro

Imre Szabo,[1] Michael R. Manning,[1] Alexander A. Radzievsky,[1] Michele A. Wetzel,[2] Thomas J. Rogers,[2] and Marvin C. Ziskin[1]*

[1]*Center for Biomedical Physics, Temple University School of Medicine, Philadelphia, Pennsylvania*
[2]*Department of Microbiology and Immunology, Temple University School of Medicine, Philadelphia, Pennsylvania*

Low power millimeter wave (LP-MW) irradiation has been successfully used in clinical practice as an independent and/or supplemental therapy in patients with various diseases. It is still not clear, however, whether exposed skin is directly affected by repeated LP-MW irradiation and whether cells of the epidermis can be activated by the absorbed energy. Keratinocytes, the most numerous component of the epidermis are believed to manifest functional responses to physical stimuli. In this study we analyzed whether LP-MW irradiation modulated the production of chemokines, including RANTES and IP-10 of keratinocytes in vitro. We also investigated whether LP-MW irradiation induces a heat stress reaction in keratinocytes, and stimulates heat shock protein 70 (Hsp70) production. Vital staining of keratinocytes with carboxyfluorescein succinimidyl ester and ethidium bromide was used to analyze the MW effect on the viability of adherent cells. In addition, we studied the effect of LP-MW irradiation on intercellular gap junctional communication in keratinocyte monolayers by Lucifer yellow dye transfer. We found no significant changes in constitutive RANTES and inducible IP-10 production following LP-MW irradiation. LP-MW exposure of keratinocyte monolayers did not alter Hsp70 production, unlike exposure to higher power MWs (HP-MW) or hyperthermia (43 °C; 1 h). LP-MW irradiation and hyperthermia did not alter the viability of adherent keratinocytes, while HP-MW irradiation induced cellular damage within the beam area. Finally, we found no alteration in the gap junctional intercellular communication of keratinocytes following LP-MW irradiation, which on the other hand, was significantly increased by hyperthermia. In summary, we detected no harmful effect of LP-MW irradiation on both keratinocyte function and structure in vitro, although these cells were sensitive to higher MW power that developed heat stress reaction and cellular damage. Our results provide further evidence that LP-MW irradiation does not induce evidence of skin inflammation or keratinocyte damage and that its clinical application appears to be safe. Bioelectromagnetics 24:165–173, 2003.

Key words: HaCaT; chemokine; heat shock protein; vital staining; gap junctional communication

INTRODUCTION

Low power millimeter wave (LP-MW) irradiation has been found to induce numerous beneficial biological effects [reviewed in Pakhomov et al., 1998] and was successfully applied in clinical practice in the past decade [Korpan and Saradeth, 1995; Pakhomov et al., 1998; Rojavin and Ziskin, 1998; Radzievsky et al., 1999]. In spite of the rising number of in vivo and in vitro studies, the nature of MW exposure on the human organism is not well understood [Pakhomov et al., 1998]. Theoretical and experimental data show that nearly all of the MW energy is absorbed in the superficial layers of skin (epidermis and dermis) [Alekseev and Ziskin, 2001a,b] suggesting that keratinocytes, the

Grant sponsor: NIH; Grant numbers: R01-AT00493, DA-11130, DA-14230, DA-06650, P30-DA-13429, T32-DA-07237, F31-DA-05894.

*Correspondence to: Marvin C. Ziskin, Center for Biomedical Physics, Temple University School of Medicine, 3400 N. Broad St., Philadelphia, PA 19140. E-mail: ziskin@astro.temple.edu

Received for review 29 January 2002; Final revision received 30 May 2002

DOI 10.1002/bem.10077
Published online in Wiley InterScience (www.interscience.wiley.com).

main constituents of epidermis, might be affected by MW exposure. Moreover, several negative skin reactions were reported following LP-MW irradiation, including cutaneous allergic reactions [Reviewed by Pakhomov et al., 1998], enhanced delayed type hypersensitivity in murin skin model [Logani et al., 1999], and morphological changes in murin skin nerves [Zavgorogny et al., 2000].

Our previous studies showed that in vitro exposure of keratinocytes to LP-MW did not modulate adhesion, proliferation, or migratory capacity of these cells, while intracellular IL-1β production was slightly increased [Szabo et al., 2001a]. In this study we further analyzed the in vitro effect of MW irradiation on epidermal keratinocytes by measuring chemokine release, heat shock protein production, determining cell viability, and gap junctional intercellular communication, in order to learn more about potential risk factors of MW exposure.

Chemokines (chemotactic cytokines) have been found to play a crucial role in cell trafficking in many physiological and pathological processes [Taub and Oppenheim, 1994; Luster, 1998; Ma et al., 1998; Locati and Murphy, 1999; Lukacs et al., 1999; McGrath et al., 1999; Murdoch and Finn, 2000]. Activated keratinocytes have been reported to produce and release several chemokines including RANTES (regulated on activation and normal T cell expressed and secreted) and IP-10 (interferon-gamma-inducible 10 kDa protein), and might initiate or augment inflammatory processes [Boorsma et al., 1998; Albanesi et al., 2000; Frank et al., 2000]. Enhanced RANTES production was found in psoriatic epidermis [Fukuoka et al., 1998; Raychaudhuri et al., 1999], while keratinocyte derived IP-10 was detected in histological samples from inflammatory skin diseases [Flier et al., 2001] and also cutaneous T cell lymphoma [Tensen et al., 1998]. In the present study we analyzed whether MW irradiation might induce activation of epidermal keratinocytes that results in the production of RANTES and IP-10, chemokines that represent potential risk factors for skin inflammation.

Stress conditions, including microbial, biochemical, or physical insults have been reported to induce heat shock protein production in live cells [Maytin, 1995; Bowman et al., 1997; Bowers et al., 1999; Miller et al., 2000; Ofenstein et al., 2000; Park et al., 2000]. Heat shock protein 70 (Hsp70) represents one of the major stress proteins essential for cellular recovery, survival, and maintenance of normal cellular function [Mayer and Bukau, 1998]. It is also a molecular chaperone that prevents protein aggregation and refolds damaged proteins in response to cellular stress caused by environmental insults, pathogens, and disease [Maytin, 1995]. We studied whether MW irradiation might induce Hsp70 production in keratinocytes in vitro comparing the effect of LP-MW, higher power MW (HP-MW) irradiation, and hyperthermia.

The vital dye carboxyfluorescein succinimidyl ester (CFSE) has been widely used in immunohistology and flowcytometry for analysis of cell viability and cell division [De Clerck et al., 1994; Hanthamrongwit et al., 1994; Lyons, 2000; May et al., 2001]. The combination of CFSE staining with ethidium bromide (EB), which counterstains dead cells, provided a reliable method for studying MW effect on cell viability in confluent keratinocyte cultures.

Epidermal keratinocytes have been found to utilize various types of cell-to-cell communication, including gap junctional intercellular communication [Salomon et al., 1988]. Gap junctions represent protein channels between two adjacent cells, allowing regulated transfer of low molecular weight substances [Bruzzone et al., 1996; Kumar and Gilula, 1996]. Using the scrape loading assay dye transfer technique to introduce the fluorescent dye Lucifer yellow into keratinocytes, the gap junctional intercellular communications were quantified by counting of stained cells [Opsahl and Rivedal, 2000]. We studied whether LP-MW irradiation might modulate dye transfer and so gap junctional intercellular communications contribute to LP-MW effect.

MATERIALS AND METHODS

Cell Culture

Spontaneously immortalized human keratinocyte HaCaT cells were a kind gift from Prof. N. E. Fusenig (University of Heidelberg, Germany). Keratinocytes were continuously cultured in RPMI-1640 medium (Gibco BRL, Grand Island, NY) with 10% FCS (HyClone, Logan, UT) (R10) at 37 °C in 5% CO_2. When required, the adherent keratinocytes were detached by using 0.05% Trypsin-EDTA (Sigma, St. Louis, MO). The cell viability during normal culture conditions was typically near 100%, as determined by the Trypan blue exclusion test.

LP-MW Exposure

Adherent keratinocytes in standard tissue culture plates were exposed from the bottom as described earlier [Szabo et al., 2001a]. The Russian made millimeter wave generator (G-141) produced a continuous wave 61.2 ± 2.1 GHz field with an output power of 20 mW that resulted in a specific absorption rate (SAR) of 770 ± 42 W/kg. Under these conditions, the steady state temperature elevation of the exposed samples never exceeded 1.6 °C. The incident power density was

calculated to be 29 ± 2 mW/cm^2 as described in our previous publication [Szabo et al., 2001a]. This type of MW irradiation was designated low power MW (LP-MW) irradiation through the manuscript.

High-Power Millimeter Wave Exposure

A Radio Research Incorporated 1 W, 42.25 GHz generator (part number 9-2-2T) was purchased and modified by the addition of a Millimetrics single junction, Q band circulator with 20 dB minimum isolation to protect the generator's Varian Klystron (VA535P) from reflected millimeter wave energy. The output of the circulator was connected through an adapter to a section of Russian wave guide with internal dimensions of 2.6 mm by 5.2 mm (13.52 mm^2 area). The power output was kept at 225 mW. The incident power density was 1.67 W/cm^2, which resulted in a peak SAR of 37 ± 3 kW/kg and a maximum temperature elevation to 45.2 °C by the end of 30 min. The SAR was calculated by multiplication of the specific heat of water ($4186\ \mathrm{J} \times \mathrm{kg}^{-1} \times \mathrm{K}^{-1}$) by the initial rate of temperature rise as determined thermographically. Reflection was measured as 0.033 ± 0.001.

During exposures, each cell culture well was placed such that the wave guide aperture was centered on, but not touching the bottom of the tissue culture well. This irradiation resulted in an exposure of 1.4% of the total keratinocyte monolayer surface. Because of the low percentage of cell being irradiated, further analyses of the cells exposed to the high power millimeter waves were limited to microscopically observable changes in the cells that were actually exposed.

Temperature Measurement

The temperature profile of HP-MW irradiation was generated by an infrared camera (Amber Engineering, Inc., Goleta, CA). The profile represents the surface temperature of the medium at the end of the 60 min HP-MW irradiation. The maximum temperature at the bottom of the tissue culture plates, where HaCaT keratinocytes were adhered, was 45.2 °C as determined by a thermocouple (Physitemp Instrument, Inc., Clifton, NJ). This area was located within a ~ 0.5 mm diameter small circle.

UVB Irradiation

Keratinocyte monolayers in 6 well tissue culture plates were irradiated by UVB light (302 nm, Chromato-Vue Lamp, San Gabriel, CA) with dish lids removed, using a dose of 150 mJ/cm^2. The UV dose was monitored with an International Light, Inc. (Newburyport, MA) radiometer fitted with a UVB detector. After irradiation keratinocyte monolayers were incubated for 24 h at 37 °C, 5% CO_2 and were stained with CFSE/EB vital staining.

Measurement of RANTES in HaCaT Supernatants

HaCaT keratinocytes (2.5×10^5 cells) in R10 were loaded into two opposite corner wells of 6 well tissue culture plates (Becton-Dickinson, Franklin Lakes, NJ). One corner well of the exposed plate was irradiated with LP-MWs at a room temperature for 30 min, while the opposite well was left as a sham control. A separate plate with keratinocytes was kept at 37 °C, 5% CO_2 for control. All plates with keratinocytes were further cultured for 24 h at 37 °C, 5% CO_2 and the supernatants were either collected or changed with fresh medium and the culture was continued for an additional 24 h.

The concentration of RANTES present in culture supernatants was determined by ELISA, using matched mouse capture and detection antibodies in a sandwich ELISA. The anti-chemokine ''capture'' antibody used in these experiments was rabbit polyclonal anti-human RANTES (Pharmingen, San Diego, CA). The capture antibody was coated onto plastic microwell plates (Nalge Co., Rochester, NY) and blocked with 1% BSA-containing PBS, and graded dilutions of culture supernatant or recombinant standard (Peprotech, Rocky Hill, NJ) were added. After washing, the captured chemokine proteins were detected using biotin-conjugated anti-chemokine ''detection'' polyclonal anti-human RANTES, followed by HRP-linked streptavidin (Vector Laboratories, Burlingame, CA). Following the addition of ABTS 2,2′-azino-bis-(3-ethylbenzthiaz oline-6-sulfonic acid) in buffer, the level of colored product was measured spectrophotometrically at 405 nm.

No detectable RANTES was found in the culture medium. The number of cells in each well was determined following detachment by Trypsin-EDTA and counting cells in hemocytometer. RANTES production was expressed in pg/10^6 keratinocytes in 24 h culture period. Each analysis was carried out in duplicate and repeated five times.

Measurement of IP-10 in HaCaT Supernatant

HaCaT keratinocytes (2.5×10^5 cells in 500 µl R-10) were loaded into two opposite corner wells of 24 well tissue culture plates (Becton-Dickinson, Franklin Lakes, NJ) and were incubated overnight at 37 °C, 5% CO_2 in order to achieve complete confluency. Then the medium was changed and one corner well of the exposed plate was irradiated with LP-MWs at room temperature for 30 min, while the opposite well was left as a sham control. The effect of MW irradiation was studied either in the presence or absence of

100 ng/ml IFNγ (Genzyme, Cambridge, MA), added to the wells before irradiation. Separate plates with keratinocytes were kept at 37 °C, 5% CO_2 for control. After irradiation, keratinocytes were further cultured for 24 h at 37 °C, 5% CO_2 and the supernatants were analyzed for IP-10 production. The IP-10 concentration in supernatants was determined by an ELISA kit (HyCult Biotechnology, Uden, The Netherlands) following the manufacturer's instructions. No detectable level of IP-10 was present in the culture medium. These experiments were repeated four times.

Hsp70 Measurement in Cell Lysates

One million HaCaT keratinocytes in 500 µl R10 were plated into two opposite corner wells of 24 well tissue culture plates. One corner well of the exposed plates was irradiated with either LP-MW or HP-MW for 60 min at room temperature, and the other well was left as sham control. Control plates with keratinocytes were either kept at 37 °C for 60 min (negative control), or incubated at 43 °C for the same period of time (positive control). After 24 h incubation at 37 °C, 5% CO_2 Hsp70 was determined in cell lysates with an enzyme immunoassay kit (StressGen, Victoria, BC, Canada) following the manufacturer's instructions. All measurements were carried out in duplicates and were repeated five times.

Vital Staining of Keratinocytes in Monolayer

The effect of in vitro exposure of keratinocyte monolayers to MWs, UVB, or heating (43 °C) on cell viability was evaluated by staining with 5,6-carboxyfluorescein diacetate, succinimidyl ester (CFSE, Molecular Probes, Eugene, OR) and EB (International Biotechnologies, New Haven, CO). CFSE develops a bright green cytoplasmic fluorescence in live cells, while dead cells show a red nuclear fluorescence with EB. For immunostaining, the culture medium was replaced by CFSE at a final concentration of 5 µM in PBS (Cellgro, Mediatech, Inc., Herndon, VA) together with 4 mM EB. Color images were taken by a digital camera (CoolSNAP cf, Roper Scientific, Trenton, NJ) attached to a fluorescence microscope (Ljumam, P8, Russia).

Scrape Loading Lucifer Yellow Transfer

HaCaT keratinocytes (3×10^6 cells in 3 ml R10) were loaded into two opposite corner wells of 6 well tissue culture plates and were cultured at 37 °C, 5% CO_2 for 24 h. By the end of the culture period keratinocyte monolayers typically reached a complete confluency. Then the medium was replaced with fresh R10, and one corner well of the exposed plates was irradiated with MW for 30 min, while the other well was left as a sham control. Control plates with keratinocytes were kept at 37 °C 5% CO_2 (negative control), or incubated at 43 °C for the same period of time (positive control). During the last 10 min exposure (and control treatment) keratinocytes were loaded with 0.1 M Lucifer yellow dye (Sigma) by scraping the monolayers with a 26 G needle. At the end monolayers were repeatedly washed with PBS, and the dye transfer was analyzed by fluorescence microscopy and quantified by counting fluorescent adjacent cells starting at the scraped border. Cells in nonscraped areas remained unstained.

Statistical Analysis

The statistical significance between groups was evaluated using the Student's *t*-test. A P value of < 0.05 was considered significant.

RESULTS

Adherent HaCaT keratinocytes were irradiated with LP-MW for 30 min and the RANTES production was measured after 24 and 48 h (Fig. 1). Under control conditions, HaCaT cells produced 315 ± 38 pg/10^6 cell of RANTES during the first 24 h incubation, which significantly decreased to 186 ± 47 pg/10^6 cell in the subsequent 24 h of culture. MW irradiation did not significantly change the constitutive RANTES production, as the RANTES level at 24 h was 279 ± 82 pg/10^6 cell and dropped to 146 ± 22 pg/10^6 cell after the second 24 h of culture. RANTES production in sham irradiated keratinocyte cultures was similar to MW irradiated cultures (222 ± 36 pg/10^6 cell at 24 h, and 153 ± 32 pg/10^6 cell at 48 h).

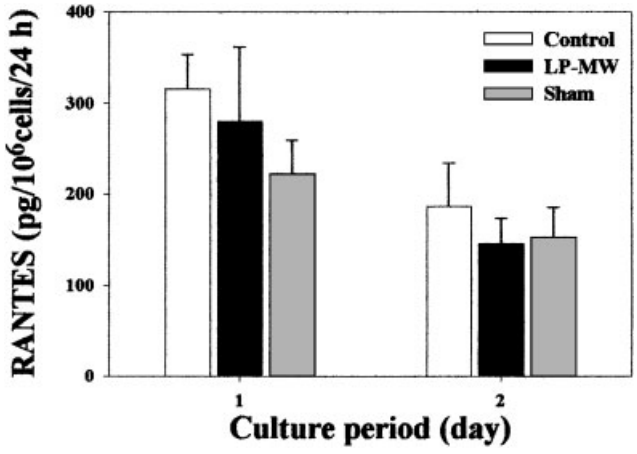

Fig. 1. The effect of LP-MW irradiation on constitutive RANTES production by HaCaT keratinocytes in vitro. Twenty-four and 48 h after irradiation, the supernatant was collected and analyzed for RANTES production by ELISA. No detectable level of RANTES was present in the culture medium. Mean ± SE of five separate experiments in duplicate.

In contrast, HaCaT keratinocytes produced very low levels of constitutive IP-10 (data not shown); however, treatment with 100 ng/ml IFNγ induced an intense IP-10 production resulting in a 1000-fold increase in IP-10 levels (Fig. 2). MW irradiated cells in the presence of IFNγ produced 5.3 ± 0.04 ng/ml IP-10, which did not significantly differ from the 5.4 ± 0.04 ng/ml IP-10 production of control cells at 37 °C, and the 5.3 ± 0.14 ng/ml production of sham irradiated cells.

In order to determine whether MW irradiation induces thermal stress reaction in keratinocytes, we measured Hsp70 production following a 60 min exposure of HaCaT cell cultures (Fig. 3). HaCaT keratinocytes were found to produce a low level of constitutive Hsp70, which was not significantly altered by LP-MW irradiation. Incubation at 43 °C, however, induced a robust increase in Hsp70 production in keratinocytes without significant alteration in cell viability (shown in Fig. 4D).

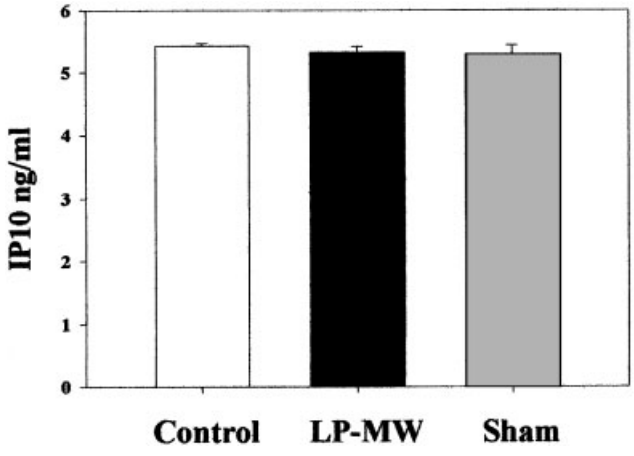

Fig. 2. The effect of LP-MW exposure on IP-10 production by keratinocytes in vitro. HaCaT keratinocytes were plated into two opposite corner wells of 24 well tissue culture plates with and without 100 ng/ml IFNγ. After 24 h incubation at 37 °C, 5% CO_2 IP-10 was measured in supernatants with ELISA. No detectable level of IP-10 was present in the culture medium. Mean ± SD of four separate experiments.

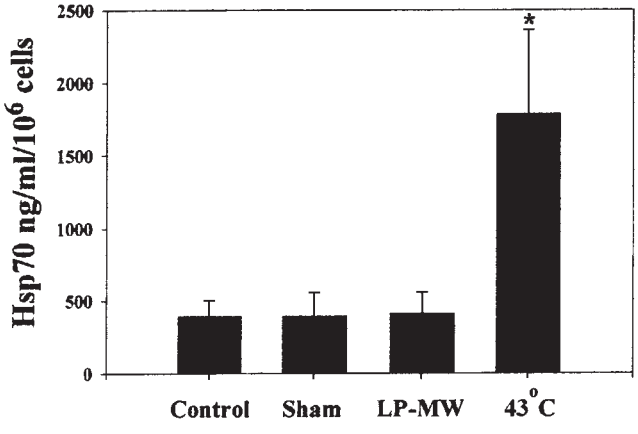

Fig. 3. The effect of millimeter wave exposure on heat shock protein 70 production in keratinocytes in vitro. After 24 h incubation at 37 °C, 5% CO_2, Hsp70 was measured in cell lysates with an enzyme immunoassay. Mean ± SD of five separate experiments in duplicate. *$P < 0.05$.

Vital staining of keratinocytes with CFSE/EB showed that keratinocyte monolayers incubated at 37 °C consist of only live cells (Fig. 4). Neither LP-MW irradiation, nor sham exposure for 60 min at room temperature caused cellular damage, as shown in Figure 4. Furthermore, incubation at 43 °C for 60 min resulted in no significant alteration in cell viability. UVB irradiation at a dose of 150 mJ/cm^2, however, caused massive cellular injury in keratinocyte cultures. The UVB treated cells exhibited fundamental changes in cell morphology and cell viability with severally damaged and dead cells. In contrast to LP-MWs, higher power MW irradiation induced severe cell damage in irradiated keratinocytes (Fig. 5). The reaction developed relatively slow, resulting in no immediate change in cell viability 1 h after irradiation (Fig. 5B). Twenty-four hours later, however, the vast majority of keratinocytes in the beam area were stained red with EB indicating severe cell damage and cell death (Fig. 5D). The cellular damage induced by HP-MW irradiation developed in the center of irradiation, where the heating effect was maximum (Fig. 6).

Keratinocytes under both in vivo and in vitro conditions develop intense cell-to-cell connections, especially when reaching a highly confluent stage. We studied whether gap junctional intercellular communications in keratinocyte monolayers were modulated by LP-MW irradiation. Keratinocytes were loaded with Lucifer yellow fluorescent dye using the scrape-loading technique. Intact cells remained unstained, while cells at the scrape margin exhibited intense dye uptake and transfer toward adjacent cells showing a gradual decrease in fluorescence intensity (Fig. 7, insert). Figure 7 shows that LP-MW irradiation resulted in no detectable modulation in gap junctional intercellular dye transfer when compared to either sham or control monolayers. Incubation at 43 °C, however, markedly increased dye travel and the number of adjacent fluorescent cells.

DISCUSSION

Application of LP-MW in clinical practice involves repeated irradiation of epidermal keratinocytes in exposed areas and might result in activation of these cells. Activated epidermal keratinocytes, however, have

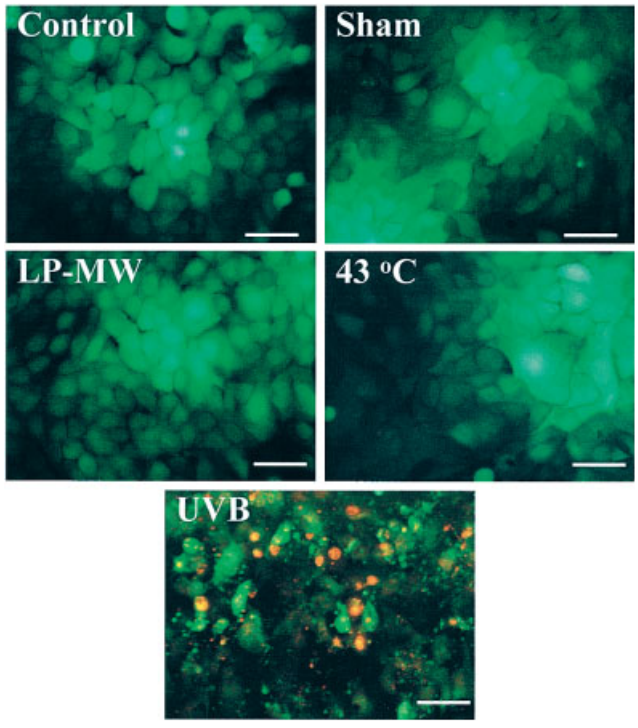

Fig. 4. The effect of MW irradiation on cell viability in keratinocyte culture. Cell viability was analyzed following 24 h culture at 37 °C, 5% CO_2 by double staining of monolayers with CFSE (green color, live cells) and EB (red color, dead cells). Scale bars on micrographs: 50 μm.

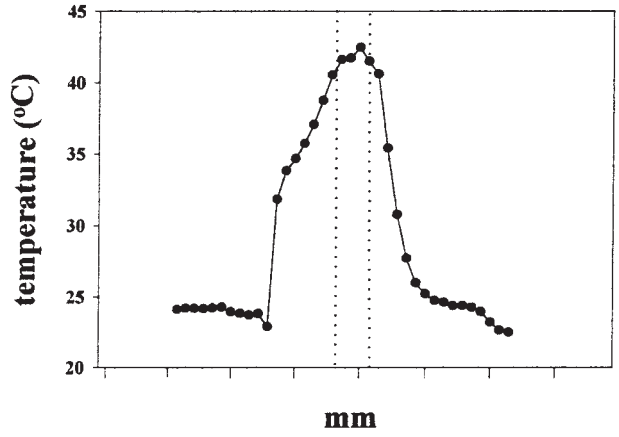

Fig. 6. Temperature profile of HP-MW irradiation. One well of a 6 well tissue culture plate containing 3 ml of culture medium was irradiated with HP-MW for 30 min from the bottom. The distribution of upper surface temperature within the beam area was determined by infrared camera at the end of irradiation. The dotted lines indicate the lateral extent of the cellular damage shown in Figure 5D.

been reported to produce a number of proinflammatory molecules including certain chemokines, which might initiate and augment inflammatory processes via attraction of immunocompetent cells into the skin [Boorsma et al., 1998; Fukuoka et al., 1998; Tensen et al., 1998;

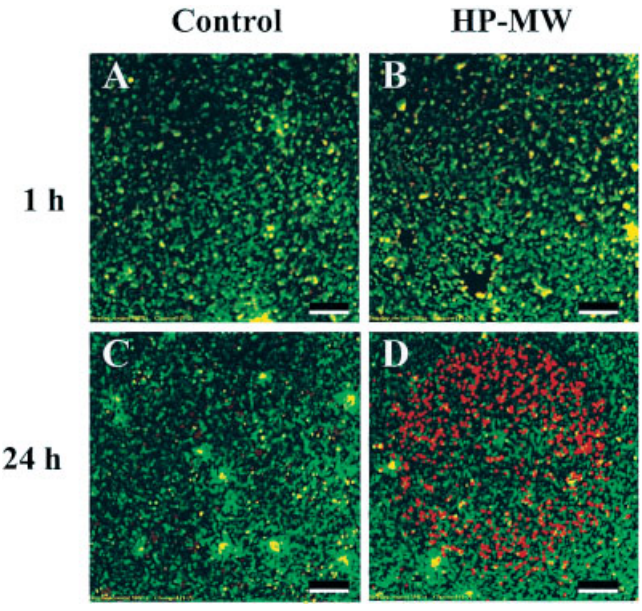

Fig. 5. The effect of HP-MW irradiation on keratinocyte viability. The cell viability was determined 1 h after irradiation (**A**, **B**) and 24 h later (**C**, **D**) by double staining of monolayers with CFSE (green color, live cells) and EB (red color, dead cells). EB positive (red) cells are located in the irradiated area. Scale bars on micrographs: 100 μm.

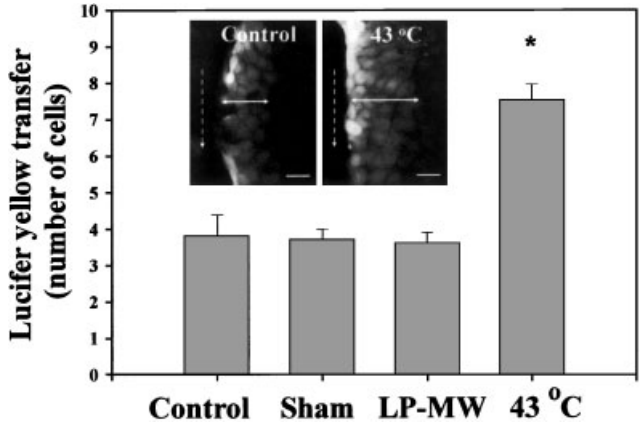

Fig. 7. The effect of LP-MW irradiation on gap junctional intercellular communication in keratinocyte monolayers. During the last 10 min of exposure (or control treatment) keratinocytes were loaded with Lucifer yellow dye by scrape-loading technique. The fluorescent microscopic images of control and 43 °C cultures are shown in inserts. Direction and localization of scraping are represented by dotted arrow-lines. The dye transfer (double arrows) was analyzed by fluorescence microscope taking color images by an attached digital camera. Keratinocytes located in the nonscraped areas remained unstained. Scale bars on micrographs: 50 μm. Quantitation of dye transfer was carried out by counting adjacent fluorescent cells starting with cells at the scrape border. Mean ± SD of five separate experiments. *$P < 0.05$.

Albanesi et al., 2000; Frank et al., 2000; Flier et al., 2001]. In an effort to determine whether LP-MW irradiation might induce or modulate the production of keratinocyte-derived chemokines, we measured the in vitro production of RANTES and IP-10, chemokines, which have been reported to play a key role in certain skin diseases. The effect of LP-MW irradiation on chemokine production was studied using HaCaT keratinocytes. These cells grow well in a serum containing tissue culture medium without addition of growth factors and show several similarities to the continuously dividing basal keratinocytes in epidermis [Boelsma et al., 1999; Schoop et al., 1999]. We have previously reported that HaCaT keratinocytes produce constitutive RANTES in a cell-density-regulated manner. We have found that in the logarithmic growth phase of cultures the RANTES production graduately decreased [Szabo et al., 2001b]. In the present study we found that LP-MW irradiation of HaCaT keratinocytes did not significantly modulate constitutive RANTES production. Moreover, the irradiated keratinocytes resembling control cells in exhibiting a similar decrease in RANTES production with propagation of cells. In contrast, HaCaT keratinocytes did not produce constitutive IP-10. In the presence of IFNγ, however, a robust level of IP-10 production was detected. LP-MW irradiation had no modulatory effect on either constitutive or inducible IP-10 production. These in vitro findings do not completely rule out the possibility of the in vivo RANTES or IP-10 production in MW exposed skin areas, but any production would certainly be far below the effective concentration level.

The biological effects of MW irradiation might involve thermal mechanisms with temperature elevation in the exposed areas [Bush et al., 1981; Walters et al., 2000]. In our previous study we detected a 1.6 °C temperature rise by LP-MW irradiation at the surface of tissue culture dishes loaded with keratinocytes [Szabo et al., 2001a]. We measured heat shock protein 70 production, one of the major heat stress proteins to determine whether MW irradiation in vitro can induce heat stress. Under control conditions HaCaT keratinocytes were found to produce a low level of Hsp70, which was not significantly altered by LP-MW exposure. HP-MW irradiation, however, induced a 29% rise in Hsp70 synthesis. The moderate rise in Hsp70 production by HP-MW irradiation was associated with the small size of irradiated area, as the wave guide used in these experiments was 5.2×2.6 mm. Moreover, we found that cellular damage induced by HP-MW irradiation was well confined within the beam area without detectable effect on cells outside the beam. Keratinocytes incubated at 43 °C for 60 min, however, produced high levels of Hsp70, and the cell viability in these cultures was not significantly altered presumably due, in part, to the protective effect of heat shock proteins produced at this temperature. Taken together these data suggest that HaCaT keratinocytes are able to respond to thermal stress with Hsp70 production. However, LP-MW irradiation induced no heat stress reaction in HaCaT cells.

Since its first introduction by Lyons and Parish [1994], the vital dye CFSE has been widely used in immunohistology and flowcytometry for analysis of cell viability or cell division [De Clerck et al., 1994; Hanthamrongwit et al., 1994; Lyons, 2000; May et al., 2001]. CFSE is a nonfluorescent dye until it enters the cells by crossing the intact cell membrane. Nonspecific cytoplasmic esterases transform the dye into a fluorescent form by a cleavage of ester groups. The active compound binds to slow turnover intracellular proteins and this conjugate might remain inside the cells for a relatively long time. The dye transformation needs intact intracellular metabolism, and is indicative of cell viability. Loaded live cells show a bright green fluorescence with fluorescent microscopy. In contrast, EB cannot penetrate through intact cell membranes, and it stains the nuclei of dead cells. Dead cells show a bright red nuclear fluorescence. The combination of CFSE staining with EB provided a reliable method to analyze the location and the magnitude of the MW effect on keratinocytes in vitro.

We found no alteration in the cell viability following LP-MW irradiation. Control cultures, or sham irradiated keratinocyte monolayers were typically composed of only live cells. UVB irradiation, however, induced severe cell damage with the characteristic phenotypical changes for apoptosis. HP-MW irradiation had no immediate effect on keratinocyte viability, however, 24 h after irradiation, the majority of cells within the beam became EB positive due to the intense cellular damage. Resistance of HaCaT keratinocytes to LP-MW irradiation and hyperthermia (43 °C) are thought to be part of the protective properties of epidermal keratinocytes. At the same time, HaCaT cells were sensitive to the effect of UVB or HP-MW irradiation, and developed severe cellular damage. Taken together, these in vitro findings do not support the possibility of keratinocyte damage in LP-MW irradiated skin areas, where the in vivo mechanisms are known to exert precise temperature regulation.

Gap junctional intercellular communications provide a relatively fast, although limited signal transfer for cells in various tissues [Bruzzone et al., 1996; Kumar and Gilula, 1996]. The role of this type of intercellular communication in epidermis is less understood [Salomon et al., 1988; Fitzgerald et al., 1994]. We found that LP-MW irradiation of confluent keratinocyte

monolayers induced no significant change in Lucifer yellow dye travel, a tracer for gap junctional communication. Incubation at 43 °C, however, markedly enhanced the number of communicating cells. These findings together with the Hsp70 data, however, are consistent with our observation that LP-MW fails to significantly elevate the temperature in irradiated cultures. In conclusion, our data support the contention that LP-MW irradiation in clinical practice is safe and without a risk of induction of topical inflammatory reactions or cell damage in epidermal keratinocytes.

ACKNOWLEDGMENTS

These studies were supported in part by NIH Grants R01-AT00493, DA-11130, DA-14230, DA-06650, P30-DA-13429, T32-DA-07237, F31-DA-05894.

REFERENCES

Albanesi C, Scarponi C, Sebastiani S, Cavani A, Federici M, De Pita O, Puddu P, Girolomoni G. 2000. IL-4 enhances keratinocyte expression of CXCR3 agonistic chemokines. J Immunol 165:1395–1402.

Alekseev SI, Ziskin MC. 2001a. Distortion of millimeter-wave absorption in biological media due to presence of thermocouples and other objects. IEEE Trans Biomed Eng 48:1013–1019.

Alekseev SI, Ziskin MC. 2001b. Millimeter wave power density in aqueous biological samples. Bioelectromagnetics 22:288–291.

Boelsma E, Verhoeven MCH, Ponec M. 1999. Reconstruction of a human skin equivalent using a spontaneously transformed keratinocyte cell line (HaCaT). J Invest Dermatol 112:489–498.

Boorsma DM, Flier J, Sampat S, Ottevanger C, de Haan P, Hooft L, Willemze R, Tensen CP, Stoof TJ. 1998. Chemokine IP-10 expression in cultured human keratinocytes. Arch Dermatol Res 290:335–341.

Bowers W, Blaha M, Alkhyyat A, Sankovich J, Kohl J, Wong G, Patterson D. 1999. Artificial human skin: Cytokine, prostaglandin, Hsp70 and histological responses to heart exposure. J Dermatol Sci 20:172–182.

Bowman PD, Schuschereba ST, Lawlor DF, Gilligan GR, Mata JR, DeBaere DR. 1997. Survival of human epidermal keratinocytes after short-duration high temperature: Synthesis of HSP70 and IL-8. Am J Physiol 272:1988–1994.

Bruzzone R, White TW, Paul DL. 1996. Connections with connexins: The molecular basis of direst intercellular signaling. Eur J Biochem 238:1–27.

Bush LG, Hill DW, Riazi A, Stensaas LJ, Partlow LM, Gandhi OP. 1981. Effects of millimeter-wave radiation on monolayer cell cultures. III. A search for frequency-specific athermal biological effects on protein synthesis. Bioelectromagnetics 2: 151–159.

De Clerck LS, Bridts CH, Mertens AM, Moens MM, Stevens WJ. 1994. Use of fluorescent dyes in the determination of adherence of human leucocytes to endothelial cells and the effect of fluorochromes on cellular function. J Immunol Methods 172:115–124.

Fitzgerald DJ, Fusenig NE, Boukamp P, Picco-li C, Mesnil M, Yamasaki H. 1994. Expression and function of connexin in normal and transformed human keratinocytes in culture. Carcinogenesis 15:1859–1865.

Flier J, Boorsma DM, van Beek PJ, Nieboer C, Stoof TJ, Willemze R, Tensen CP. 2001. Differential expression of CXCR3 targeting chemokines CXCL10, CXCL9, and CXCL11 in different types of skin inflammation. J Pathol 194:398–405.

Frank S, Kampfer H, Wetzler C, Stallmeyer B, Pfeilschifter J. 2000. Large induction of the chemotactic cytokine RANTES during cutaneous wound repair: a regulatory role for nitric oxide in keratinocyte-derived RANTES expression. Biochem J 1:265–273.

Fukuoka M, Ogino Y, Sato H, Ohta T, Komoriya K, Nishioka K, Katayama I. 1998. RANTES expression in psoriatic skin, and regulation of RANTES and IL-8 production in cultured epidermal keratinocytes by active vitamin D3 (tacalcitol). Br J Dermatol 138:63–70.

Hanthamrongwit M, Reid WH, Courtney JM, Grant MH. 1994. 5-Carboxyfluorescein diacetate as a probe for measuring the growth of keratinocytes. Hum Exp Toxicol 13:423–427.

Korpan NN, Saradeth T. 1995. Clinical effects of continuous microwave for postoperative septic wound treatment: A double-blind controlled trial. Am J Surg 170:271–276.

Kumar NM, Gilula NB. 1996. The gap junction communication channel. Cell 84:381–388.

Locati M, Murphy PM. 1999. Chemokines and chemokine receptors: Biology and clinical relevance in inflammation and AIDS. Annu Rev Med 50:425–440.

Logani MK, Yi L, Ziskin MC. 1999. Millimeter waves enhance delayed-type hypersensitivity in mouse skin. Electro Magnetobiol 18:165–176.

Lukacs NW, Hogaboam C, Campbell E, Kunkel SL. 1999. Chemokines: Function, regulation and alteration of inflammatory responses. Chem Immunol 72:102–120.

Luster AD. 1998. Mechanisms of disease: Chemokines-chemotactic cytokines that mediate inflammation. N Eng J Med 338: 436–445.

Lyons AB. 2000. Analysing cell division in vivo and in vitro using flow cytometric measurement of CFSE dye dilution. J Immunol Methods 243:147–154.

Lyons AB, Parish CR. 1994. Determination of lymphocyte division by flow cytometry. J Immunol Methods 171:131–137.

Ma Q, Jones D, Borghesani PR, Segal RA, Nagasawa T, Kishimoto T, Bronson RT, Springer TA. 1998. Impaired B-lymphopoiesis, myelopoiesis, and derailed cerebellar neuron migration in CXCR4- and SDF-1-deficient mice. Proc Natl Acad Sci USA 95:9448–9453.

May AL, Wood FM, Stoner ML. 2001. Assessment of adhesion assays for use with keratinocytes. Exp Dermatol 10:62–69.

Mayer MP, Bukau B. 1998. Hsp70 chaperone systems: Diversity of cellular functions and mechanism of action. Biol Chem 379: 261–268.

Maytin EV. 1995. Heat shock proteins and molecular chaperones: Implication for adaptive responses in the skin. J Invest Dermatol 104:448–455.

McGrath KE, Koniski AD, Maltby KM, McGann JK, Palis J. 1999. Embryonic expression and function of the chemokine SDF-1 and its receptor, CXCR4. Dev Biol 213:442–456.

Miller CM, Akratos C, Johnson AM, Smith NC. 2000. The production of a 70 kDa heat shock protein by Toxoplasma gondii

RH strain in immunocompromised mice. Int J Parasitol 30: 1467–1473.
Murdoch C, Finn A. 2000. Chemokine receptors and their role in vascular biology. J Vasc Res 37:1–7.
Ofenstein JP, Heidenamm S, Juett-Wilstermann A, Sarnaik A. 2000. Expression of stress proteins HSP 72 and HSP 32 in response to endotoxemia. Ann Clin Lab Sci 30:92–98.
Opsahl H, Rivedal E. 2000. Quantitative determination of gap junction intercellular communication by scrape loading and image analysis. Cell Adhes Commun 7:367–375.
Pakhomov AG, Akyel Y, Pakhomova ON, Stuck BE, Murphy MR. 1998. Current state and implications of research on biological effects of millimeter waves: A review of the literature. Bioelectromagnetics 19:393–413.
Park SH, Lee SJ, Chung HY, Kim TH, Cho CK, Yoo SY, Lee YS. 2000. Inducible heat-shock protein 70 is involved in the radioadaptive response. Radiat Res 153:318–326.
Radzievsky AA, Rojavin MA, Cowan A, Ziskin MC. 1999. Suppression of pain sensation caused by millimeter waves: A double-blinded, cross-over, prospective human volunteer study. Anesthesia Analgesia 88:836–840.
Raychaudhuri SP, Jiang WY, Farber EM, Schall TJ, Ruff MR, Pert CB. 1999. Upregulation of RANTES in psoriatic keratinocytes: A possible pathogenic mechanism for psoriasis. Acta Derm Venereol 79:9–11.
Rojavin MA, Ziskin MC. 1998. Medical application of millimeter waves. Quarterly J Med 91:57–66.
Salomon D, Saurat JH, Meda P. 1988. Cell-to-cell communication within intact human skin. J Clin Invest 82:248–254.
Schoop VM, Mirancea N, Fusenig NE. 1999. Epidermal organization and differentiation of HaCaT keratinocytes in organotypic coculture with human dermal fibroblasts. J Invest Dermatol 112:343–353.
Szabo I, Rojavin MA, Rogers TJ, Ziskin MC. 2001a. Reactions of keratinocytes to in vitro millimeter wave exposure. Bioelectromagnetics 22:358–364.
Szabo I, Wetzel MA, Rogers TJ. 2001b. Cell density-regulated chemotactic responsiveness of keratinocytes in vitro. J Invest Dermatol 117:1083–1090.
Taub DD, Oppenheim JJ. 1994. Chemokines, inflammation and the immune system. Ther Immunol 1:229–246.
Tensen CP, Vermeer MH, van der Stoop PM, van Beek P, Scheper RJ, Boorsma DM, Willemze R. 1998. Epidermal interferon-gamma inducible protein-10 (IP-10) and monokine induced by gamma-interferon (Mig) but not IL-8 mRNA expression is associated with epidermotropism in cutaneous T cell lymphomas. J Invest Dermatol 111:222–226.
Walters TJ, Blick DW, Johnson LR, Adair ER, Foster KR. 2000. Heating and pain sensation produced in human skin by millimeter waves: Comparison to a simple thermal model. Health Phys 78:259–267.
Zavgorogny SV, Khizhnyak YP, Voronkov VN, Sadovnikov VB. 2000. Morphological changes in skin nerves caused by electromagnetic radiation of millimeter range. Crit Rev Biomed Eng 28:641–658.